

# Application of microneedle patches for drug delivery; doorstep to novel therapies

Journal of Tissue Engineering  
Volume 13: 1–25  
© The Author(s) 2022  
Article reuse guidelines:  
sagepub.com/journals-permissions  
DOI: 10.1177/20417314221085390  
journals.sagepub.com/home/tej



Fateme Nazary Ahrbekoh<sup>1</sup>, Leila Salimi<sup>1</sup>,  
Sepideh Saghati<sup>1</sup> , Hassan Amini<sup>1</sup>,  
Sonia Fathi Karkan<sup>1</sup> , Keyvan Moharamzadeh<sup>2</sup>,  
Emel Sokullu<sup>3</sup> and Reza Rahbarghazi<sup>1,4</sup>

## Abstract

In the past decade, microneedle-based drug delivery systems showed promising approaches to become suitable and alternative for hypodermic injections and can control agent delivery without side effects compared to conventional approaches. Despite these advantages, the procedure of microfabrication is facing some difficulties. For instance, drug loading method, stability of drugs, and retention time are subjects of debate. Besides, the application of novel refining fabrication methods, types of materials, and instruments are other issues that need further attention. Herein, we tried to summarize recent achievements in controllable drug delivery systems (microneedle patches) *in vitro* and *in vivo* settings. In addition, we discussed the influence of delivered drugs on the cellular mechanism and immunization molecular signaling pathways through the intradermal delivery route. Understanding the putative efficiency of microneedle patches in human medicine can help us develop and design sophisticated therapeutic modalities.

## Keywords

Microneedle patches, transdermal injection, drugs, delivery system, diabetes

Date received: 6 January 2022; accepted: 17 February 2022

## Introduction

During the last decades, numerous attempts have been made to deliver recommended dose of drugs and therapeutic compounds to the target tissues with fewer side effects.<sup>1,2</sup> Due to ease of access and less invasive manipulation, transdermal delivery of target molecules has been at the center of attention.<sup>1,2</sup> This approach is a newly generated delivery route system that solves previous disadvantages such as pain, patient anxiety, low dose delivery, and other side effects.<sup>3</sup> Besides, the transdermal delivery route has diminished the possible biodegradation of drugs inside the gastrointestinal tract and through hepatic activity. Despite these advantages, cutaneous tissue develops a substantial barrier against multiple foreign agents with specific physicochemical properties. The epidermal layer is the first target surface for the transdermal delivery route to release the target compound into the blood circulation.<sup>4-6</sup>

It was suggested that lipophilic compounds with low molecular weight (<500 Da) can easily cross the epidermal layer; however, it is difficult for pharmaceutical bio-macromolecules and other biomolecules such as nucleic acids or

<sup>1</sup>Stem Cell Research Center, Tabriz University of Medical Sciences, Tabriz, Iran

<sup>2</sup>Hamdan Bin Mohammed College of Dental Medicine, Mohammed Bin Rashid University of Medicine and Health Sciences, Dubai, United Arab Emirates

<sup>3</sup>Koç University Research Center for Translational Medicine (KUTTAM), Istanbul, Turkey

<sup>4</sup>Department of Applied Cell Sciences, Faculty of Advanced Medical Sciences, Tabriz University of Medical Sciences, Tabriz, Iran

### Corresponding author:

Reza Rahbarghazi, Tabriz University of Medical Sciences, Imam Reza Hospital, Daneshgah Street, Tabriz 51666-14756, Iran.  
Emails: reza.rahbarghazi@gmail.com; rahbarghazi@tbzmed.ac.ir



proteins, to reach deeper layer of skin. In line with this claim, both passive and active methods have been applied to increase transdermal delivery of target compounds.<sup>7</sup> In the passive methods, optimized drug formulation or application of carriers often leads to restricted transfer of biomacromolecules. By contrast, the application of active physical or mechanical modalities yields outstanding skin permeability, even for compounds with higher molecular weights.<sup>8</sup> For instance, several microneedles (MN) with different needle lengths (from 100 to 1100  $\mu\text{m}$ ) and needle densities per  $\text{cm}^2$  have been fabricated for different purposes. Of note, the local application of MN containing needle in 100–700  $\mu\text{m}$  length can generate micro-sized channels through the stratum corneum, leading to facilitated delivery of target molecules to the target sites. Based on histological studies, the average thickness of the stratum corneum is about 10  $\mu\text{m}$ .<sup>9</sup> It should not be forgotten the fact that the chemical properties of certain drugs can be affected using direct conventional transdermal administration which per se restricts further absorption through the subcutaneous layer into the systemic circulation.<sup>10</sup> Development of sophisticated delivery systems such as MN not only can increase the delivery efficiently but also reduce the total dose of medication. Some features such as the dissolving rate of needles can also vary bioavailability rate. As a correlate, modification of needle geometry and size can help us to increase the deeper transdermal release of drugs. Besides, the application of water-soluble formulations or localization of biopharmaceutical agents juxtaposed to needle tips way from the basement could also stimulate drug bioavailability.<sup>11</sup> Besides, different geometrical values such as needle side wall thickness, needle height, and tip radii, as well as aspect ratio are identical in the fabrication and delivery of various compounds into the deeper layer of cutaneous tissue.

A higher aspect ratio (needle height/width ratio) can result in the development of painless MN during insertion into the cutaneous tissue while an excessive aspect ratio diminishes mechanical strength.<sup>12</sup> Because of the direct application of transdermal patches, other issues such as mechanical rigidity, loading capacity of needles, responsiveness to external stimuli, and low probability of pain should be considered.<sup>13</sup>

To date, several physical penetration enhancers such as MN, iontophoresis, electroporation, sonophoresis, ablative laser microporation, and chemical penetration enhancers like fatty acids, alcohols, esters, etc. have been used to increase delivery efficiency through the transdermal route.<sup>14,15</sup> The chemical penetration enhancers are easy to be produced in various chemical structures and are applicable without additive tools and professional clinicians. However, the chemical penetration approach may enhance the risk of severe skin inflammation especially when hydrophilic molecules are used for accelerating the delivery of therapeutic molecules.<sup>15</sup> In contrast, the physical

penetration enhancers provide a less invasive platform for fast and adjustable dose drug delivery.<sup>16</sup> Among them, the iontophoresis method is based on voltage gradient delivery of therapeutic agent through stratum corneum, the outer layer of the epidermis, by creating nano-sized holes.<sup>17</sup> It has been suggested that this approach is more appropriate for the delivery of lipophilic and small size molecules.<sup>18</sup> The efficiency of iontophoresis-based delivery is associated with the loaded drug concentration, pH of drug solution, ionic component, and physicochemical conditions.<sup>19</sup> In the sonophoresis method, ultrasound waves are exploited to improve skin permeability by increasing the local temperature and applying mechanical longitudinal force for transdermal delivery.<sup>16</sup> Although sonophoresis is known to be safe, cheap, and functional, the heating effects can alter the therapeutic effects of thermal-sensitive molecules during transdermal delivery.<sup>20</sup> However, sonophoresis also stimulates skin permeability via non-thermal approaches by tethering generated microbubble through ultrasound waves.<sup>21</sup> Electroporation supports transdermal delivery using high-voltage electric pulses based on membrane rearrangement and pore formation.<sup>22</sup> Ideally, the electroporation pulses can also induce an immune response within transdermal delivery (notably through vaccine delivery). However, the unprogrammed number of pulses and treatment elongation may cause severe damage to keratinocyte and resident cells.<sup>23</sup> In ablative laser microporation, skin resurfacing is done by laser irradiation which facilitates topical absorption and further systemic delivery to remote sites.<sup>24</sup> Similar to the other physical penetration enhancers, ablative laser facilitates the transdermal delivery of high molecular weight and hydrophilic molecules. The drug absorption can be interrupted if laser irradiation forms a large-scale coagulation area in the damaged tissue around microchannels.<sup>25,26</sup>

Recently, MN devices equipped with an array of needles with a size of less than 500  $\mu\text{m}$  have been developed for efficient delivery through an epidermal barrier (Figure 1). One of the most prominent advantages of the MN system would be that both small- and large-sized molecules such as nucleic acids, proteins, vaccines, hormones, nanoparticles, and virus-like particles can be loaded in MN devices.<sup>27–29</sup> MN devices enhance patient compliance because of painless injections while preventing in situ infections caused by conventional needles. However, the development of novel micro-fabrication methods and stability drugs inside the MN devices are still challenging. Even though the MN system has excellent potential to be an alternative to traditional methods, it can contribute to skin irritation or allergic reactions.<sup>30</sup> Progress in the development of MN devices has increased hopes for using less specialized personnel worldwide by creating self-health administration opportunities.<sup>31,32</sup>

This review initially summarizes MN fabrication methods and the application of different MN types, as delivery systems, in regenerative medicine. MN delivery system

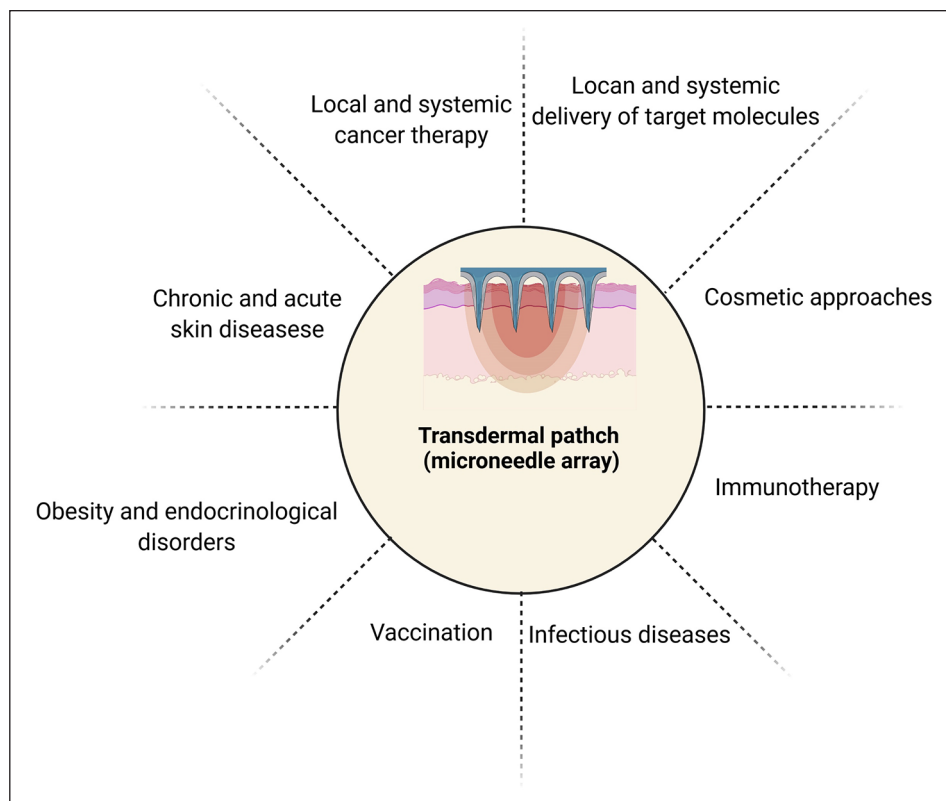


**Figure 1.** Available approached purposed for transdermal delivery using MN patch system.

utilities to target common disorders such as metabolic disorders, humoral disorders, and autoimmune disorders are also discussed. Likewise, recent progress on sophisticated therapeutic trends for virus and bacterial infections and cancer immunotherapy via MN vaccine delivery systems were also covered in this review.

### MN fabrication methods

Up to now, different types of MNs (solid, coated, hallow, and dissolving MNs) have been developed for drug delivery purposes. To fabricate MNs, materials such as hydrogels, silica glass, silicon, metals, polymers, ceramics, etc. can be used. Although MN fabrication methods are growing fast (Figure 2(a)) the most common MN fabrication methods are bulk micromachining, surface micromachining, and LIGA. During Bulk micromachining, a favorable shape is designed by substrate elimination.<sup>33</sup> Despite bulk micromachining, in surface micromachining, the shape of the substrate is developed by forming on the surface.<sup>33</sup> The etching is a common subset of bulk micromachining and surface micromachining processes. During etching, substrates are patterned by various lithographic methods like photolithography which are obtained by eliminating substrates on or in the target surface (Figure 2(b)).<sup>33–35</sup> However, photolithography has been limited by issues such as high purchasing processes and less authority in

picking materials.<sup>36</sup> RIE is a type of dry etching method and this procedure utilizes reactive plasma such as ionized gas to discard materials uncovered by a mask which leads to more accurate etching in comparison to wet etching.<sup>37,38</sup> Compared to dry etching, in wet etching, the substrate elimination is done by a chemical agent and provided both a cheap and simple fabrication process (Figure 2(a)).<sup>34,39</sup>

The LIGA process consists of metal deposition on patterned substrates.<sup>34,35,40,41</sup> X-ray or UV irradiations are commonly used for pattern stabilization. Previous experiments have successfully applied specific materials such as PMMA as a sensitive polymer in the X-ray LIGA process. Noteworthy, in UV-LIGA, an epoxy-based negative photoresist such as SU-8 is used as a photo-resistant polymer.<sup>34,35,40,41</sup> On this basis, the target metal is deposited on the resisted area without a covered mask. Finally, the photoresist material is peeled off to obtain the final desirable structure. The LIGA process is applicable for both mold fabrication and direct metal deposition. Even though X-ray LIGA is expensive and requires complex instruments compared to the UV-LIGA technique.<sup>39</sup>

Micromolding is another method in which patterned PDMS is used as a mold for substrates and an alternative that solves photolithography limitations (Figure 3).<sup>35,36</sup> Micromolding is a cheap and common process for MN fabrication; however, fractions of the loaded drug may waste during this process.<sup>42</sup> Laser irradiation such as excimer laser

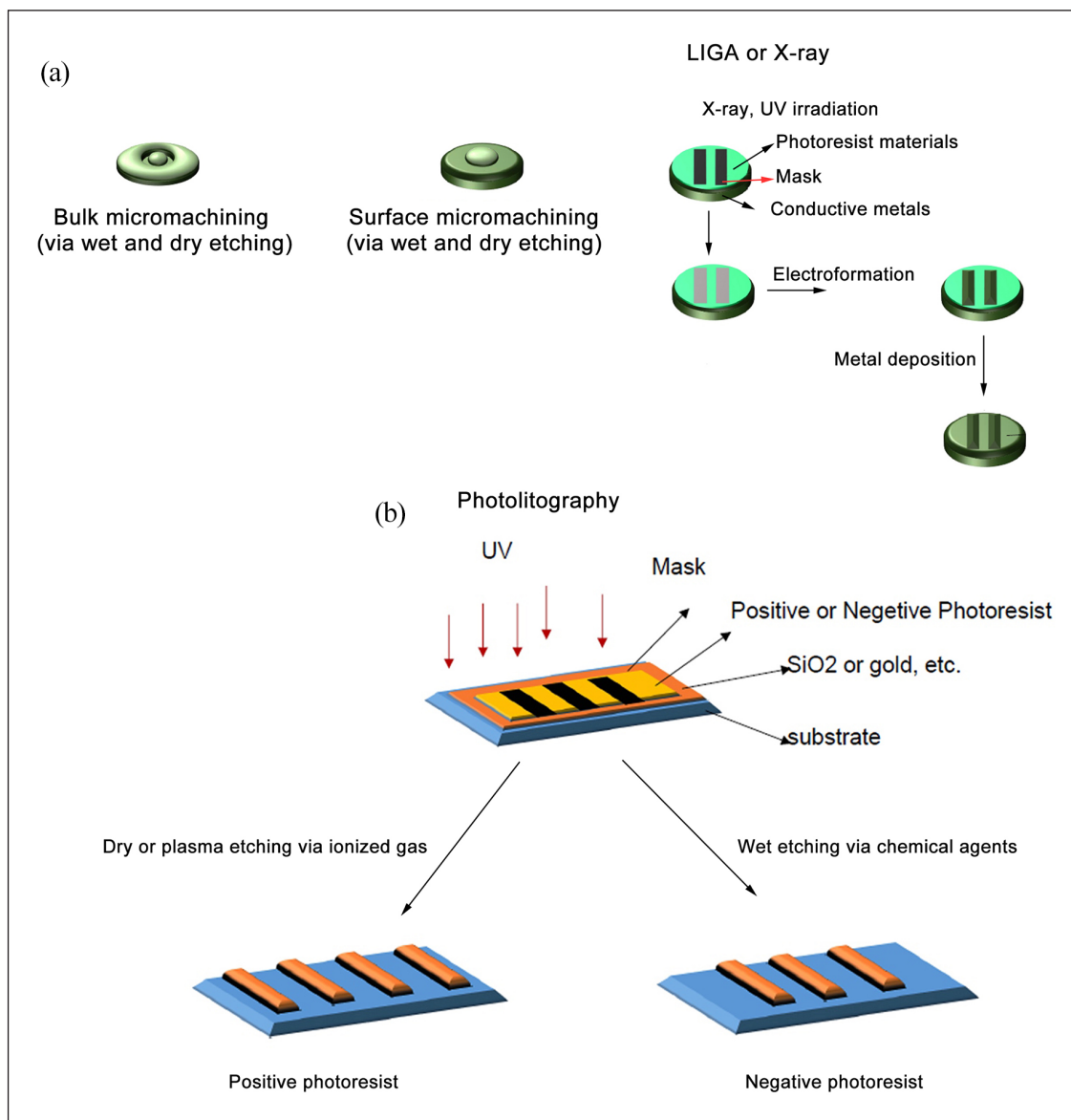


**Figure 2.** (a) MN fabrication methods are a subset of micro-electro-mechanical fabrication processes that diverged into three major groups: bulk micromachining, surface micromachining, and LIGA. (b) Photolithography process is one of the methods to the pattern desired figures on biomaterials, subsequently creating the 3D shape via wet or dry etching.

can help us to produce precise microchannels on suggested soft materials utilizing as a template for MN fabrication.<sup>43,44</sup> Meanwhile, the MN production by laser is time-consuming and it is thought that the laser irradiation is mostly suitable to design surface topography in fabrication microfluidic devices.<sup>39,44</sup> Notably, current advances in MN fabrication have led to the application of sophisticated technologies such as personalized 3D printing.<sup>45</sup> Due to the availability of specific synthesis methods, the physicochemical properties of MN devices can be adapted according to the type of target molecules and injection site. As MNs create micro-sized channels in the epidermis layer, the type, shape, size, density, and length of needles should be carefully considered.<sup>46</sup> The close association between MN geometry and effective

insertion has been shown that an increase in insertion depth of needle affects both deflections of the skin. Under these circumstances, maximum force is applied to the needle insertion due to reducing the shear forces. However, the speed of the needle penetrating did not affect the force or deflection of the skin during penetration.<sup>47,48</sup> Generally, a smaller tip diameter and tip angle and a high height to base width ratio can result in successful needle insertion.<sup>49</sup> An optimal number of needles array is critical to enhancing drug delivery and insufficient needles reduce the delivery volume. In contrast, too many needles will reduce the penetration capacity and efficiency rate. If needle penetration does not reach the targeted depth, the treatment becomes less effective due to lower concentrations in the critical

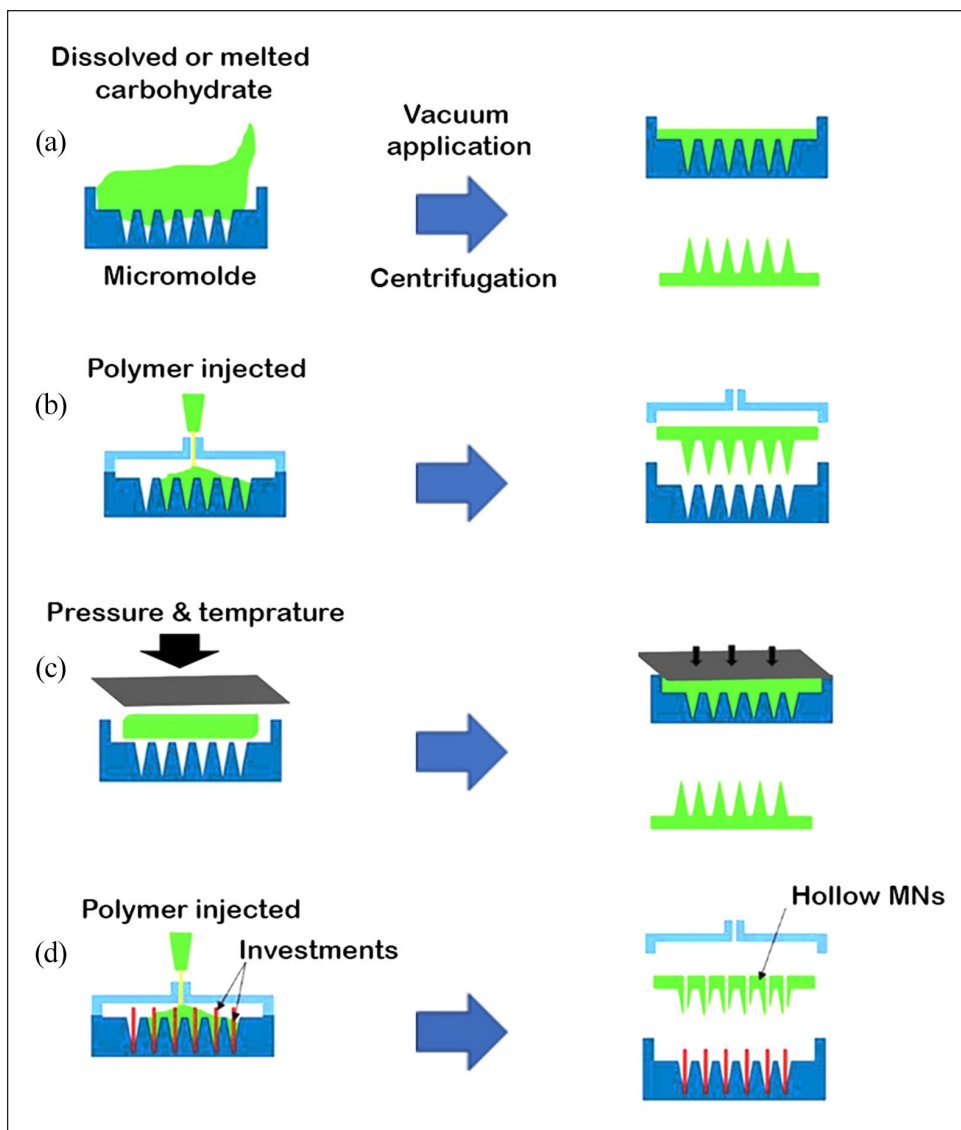


**Figure 3.** Several micromolding-based MN fabrication techniques: (a) micromolding, (b) injection molding, (c) hot embossing, and (d) investment molding.

region and leakage out of the injection site.<sup>50</sup> However, further knowledge is necessary to design MNs rationally before their fabrication, particularly to determine the most effective MN geometries and application methods and to produce a uniform and reproducible MN penetration. Nevertheless, most researchers have been seeking to optimize the MN fabrication methods and applications for different pathologies (Figure 2).

## Types of MN devices

### Solid and coated MNs

Solid MNs are usually made of silicon, ceramic, metals like gold, nickel, titanium, and non-degradable polymers with high resilience to physically form pores through the

skin, enhancing the permeability for drugs at the site of application (Figure 4).<sup>51</sup> Petchsangsaï et al.<sup>52</sup> fabricated a homemade MN array by cutting nine acupuncture needles and positioning them on a silicon matrix. They found that the use of an external insertion force of about 10 N facilitated the delivery of hydrophilic macromolecule in MNs more than the electroporation, and sonophoresis techniques, separately.<sup>52</sup> Of note, the combination of MN devices with electroporation, sonophoresis, and simultaneous electroporation-sonophoresis approaches increased the amount of delivery more than the MN system alone over 24 h.<sup>52</sup> Histological staining showed that the cutaneous tissue remained intact after treatment. Although the volatile input voltage, intensity and duration of electroporation, and sonophoresis should be examined, and safe amounts are chosen.<sup>52</sup> To increase the delivery rate, solid

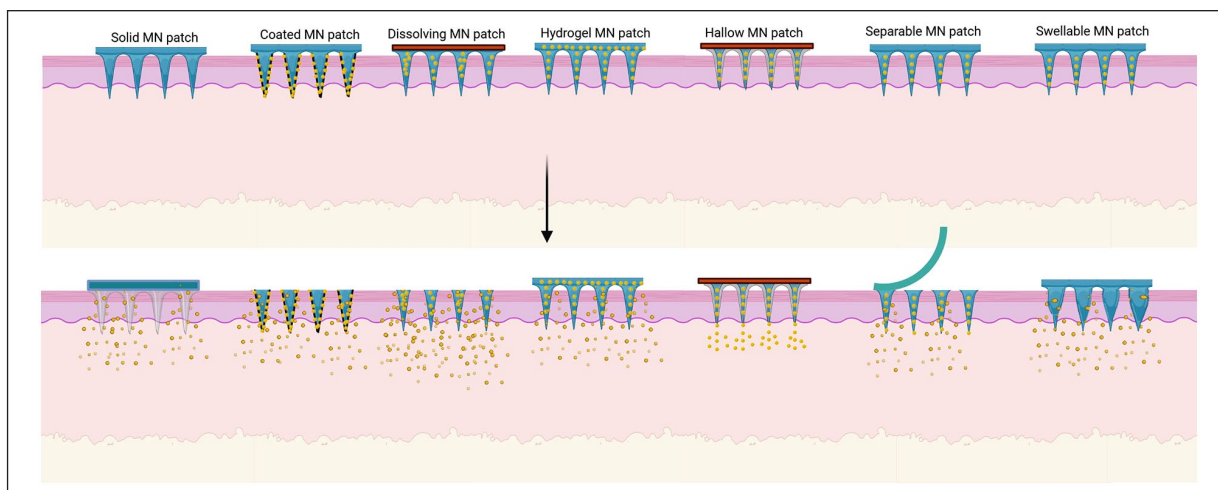


**Figure 4.** Types of MNs with different releasing mechanisms.

MNs can be coated with drug-loaded biodegradable materials with various methods like dip coating, drop coating, spray coating, layer by layer coating (based on electrostatic bond formation between surface-modified MN or pre-coated additional material and drug-loaded material).<sup>53</sup> Ideally, the coating process should provide a uniform, thin layer of drug-loaded biocompatible material on the solid MN to obtain reliable results through treatment.<sup>51</sup> Additionally, coated-MNs support various drug delivery possibilities in the one-treatment procedure of each needle in different drug solutions.<sup>1</sup> Previously, Hu et al.<sup>46</sup> constructed a metallic glass solid MN by thermoplastic drawing technique. The needles were dip-coated in red-colored drug solution to examine in vitro drug delivery potential on porcine cutaneous tissue. According to their findings, this technique is efficient for on-demand drug delivery. Besides, the developed MNs had proper mechanical, morphological, and biocompatible features to penetrate the skin and overcome skin elasticity.<sup>46</sup> In another study, Kapoor et al.<sup>54</sup> fabricated solid polymeric MN coated with  $\sim 250 \mu\text{g}$  peptide A on a  $1.27 \text{ cm}^2$  patch containing 316 needles and claimed that this system is capable of delivering target protein similar to subcutaneous administration. They also claimed that the coating procedure can stabilize peptide A, enhance protein activity, and reduce required total peptide dose loading on MN, making MN a non-invasive approach to transdermal delivery of peptides.<sup>54</sup>

### Dissolving MNs

Compared to solid MNs, dissolving MNs are fabricated by encapsulated drug-loaded biodegradable materials like polyesters, polyvinyl, and carbohydrates (Figure 4).<sup>51</sup> Whereas the solid MNs stiffness increases fracture possibility and further skin inflammation raised by broken needles, the dissolving MNs are strong enough to penetrate the skin but not as much as the solid MNs.<sup>12</sup> Dissolving

MNs regulate drug-releasing upon matrix degradation, enhance the amount of drug loading, and resolve homogeneous coating process difficulty in comparison with coated MNs.<sup>1,3,51</sup> Noteworthy, dissolving MNs might deliver the right amount of drug dose in contrast to solid and coated MNs. They are also suspected of demolition against dampened environment regard to their soluble matrix that diminished the stability rate of the designed dissolving MN.<sup>55</sup> Previously, Castilla-Casadiego et al.<sup>56</sup> designed dissolving chitosan-based MN for delivering meloxicam as a pain-relieving in cattle. Meloxicam is a nonsteroidal anti-inflammatory drug that prohibits the activity of COX-2 and prostaglandin  $E_2$ . These elements are important factors in pain sensation, vasodilation, leukocyte adhesion, inflammatory responses to TNF- $\alpha$ , and other cytokines.<sup>57</sup> They also found that the MN patch could deliver meloxicam efficiently for a week.<sup>56</sup> In another study, Ramalheiro et al. fabricated rapidly dissolving poly (vinylpyrrolidone) and poly (vinyl alcohol) MNs for the delivery of rapamycin for psoriasis purposes. To this end, they enriched phytantriol-based cubosome-like liquid crystalline with rapamycin. The loaded drug was continuously released for 14 days in in vitro conditions.<sup>58</sup> Psoriasis is a chronic inflammation of cutaneous tissue and is indicated with hyperkeratosis and abnormal thickening of the dermal layer. In addition to the proliferation of epidermal cells, the recruitment of immune cells into the affected sites is evident in histopathological examinations.<sup>59,60</sup> The presence of Th1 and T17 subsets contribute to the production of several cytokines such as TNF- $\alpha$ , IFN- $\gamma$ , IL-17A, IL-22.<sup>59,60</sup> The inhibition of mTOR is touted to participate in the regulation of autophagy, and cytoskeleton organization, cellular metabolism, and cell growth.<sup>61</sup> The release of rapamycin via dissolving MNs led to inhibition of NK cells activity and suppression of inflammation.<sup>58</sup> It seems that dissolving MNs can be used for immunomodulation in the context of cutaneous tissue.

Detachable (separable) MNs, belonging to dissolving MNs, are known to circumvent problems associated with the possible immune response following needle degradation as seen in dissolving MNs because of long-term replacement inside the cutaneous layer (Figure 4).<sup>51</sup> These MN types can quickly deliver a favorable amount of targeted drugs into the target sites. The solid backbone of separable MNs is made of non-degradable materials while arrowhead tips are fabricated using degradable scaffolds.<sup>51</sup> Pukfukdee et al.<sup>62</sup> designed a separable hyaluronic acid-polyvinylpyrrolidone-maltose as a solid matrix for cell delivery into the cutaneous tissue. In this regard, they encapsulated murine melanoma cells (B16-F10) and found the successful delivery of melanoma cells by cell-loaded needles into the hypodermic region.<sup>62</sup> Data showed cells delivery via dissolving MN with bigger tumor-sized on the dorsal back skin of experimental mice compared to hypodermic injection. The neoplastic features of cells in the two approaches were similar.<sup>62</sup> In a study, it was found that encapsulation of phyto-compound Capsaicin inside PCL needles decreased cancer cells proliferation and promoted cellular apoptosis depending on the dose concentration. The base of needles was fabricated using PVP and PVA.<sup>63,64</sup> Recently, experiments demonstrated that Capsaicin can arrest cell cycle by eliciting cyclin-dependent kinase inhibitor P21 and inhibition of ERK1/2 signaling pathways, leading to decreased cell proliferation and promoted apoptosis via JNK activation.<sup>64</sup> Eum and co-workers successfully released Capsaicin using PCL needles for consecutive 15 days. Data showed that needles composed of biodegradable and biocompatible polymers like PCL can be used instead of hydrophobic polymers for trans-dermal delivery.<sup>63</sup> In an experiment conducted by Li and co-workers, a separable polyester kind patch was fabricated with a bubble technique. This technique supports immediate separation and effective insertion which is useful for contraceptive hormone delivery. In this approach, serum levels of contraceptive hormones were increased for a month.<sup>65</sup>

### Hallow MNs

Hallow MNs are an alternative route for hypodermic delivery of high molecular weight compounds such as nucleic acids, antibodies, and proteins with large amounts. The compound release rate and pressure can be modulated by regulating the hallow size. Hollow MNs are synthesized using metals like gold, titanium, stainless steel, ceramic, and other non-degradable polymers (Figure 4).<sup>51,66</sup> The fabricated drug-loaded MNs should be examined in terms of physicochemical properties, content, rate of release, and cytotoxicity of the drug. The backbone of hallow MNs should be characterized in morphology, mechanical properties, and quality of skin permeation. The safety analyses include cutaneous tissue irritation, infection, and pain.<sup>1,14,67,68</sup> In a recent study, Cárcamo-Martínez et al.<sup>69</sup>

tried to deliver JAK inhibitor, tofacitinib citrate, intradermally for the suppression of cutaneous inflammation via hollow MN arrays composed of Gantrez<sup>®</sup> S-97 and 10% PEG, and results were compared to hallow MN system and commonly topical administration. Using neonatal porcine skin, they delivered 1393, 2158, 5685  $\mu\text{g}$  tofacitinib citrate after 24 h using the topical cream, hallow, and dissolving MN systems, respectively. They pointed out that the hallow MN supports less drug loading and the delivery rate is slower.

### Swellable MNs

Swellable MNs are specific kinds of MNs that are expanded following exposure to the cutaneous interstitial fluid (Figure 4).<sup>51,66</sup> Like other MN types, swellable MNs also provide microchannels on the skin for other drug delivery.<sup>66,70</sup> Swellable MNs are composed of hydrophilic polymers with high swell capacity such as polyethylene glycol, acrylate derivatives, etc.<sup>51,66</sup> It seems the addition of other techniques can improve the hydrophilicity of MNs. For instance, Chew et al.<sup>71</sup> improved the hydrophilicity of PEGDA polymer after cross-linking with hyaluronic acid and use of UV irradiation. The MN attachment capability was also enhanced by the coating with photo-curable materials. According to their findings, the synthesized matrix was swelled quickly in a short duration of almost 10 min in which 90% loaded drug was released to the aqueous phase. In this scenario, this platform provides high concentrate drug loading and an efficient delivery rate after the MN fabrication process.<sup>71</sup> Yang et al.<sup>72</sup> previously designed swellable MN to facilitate the sustainable release of granisetron, an antagonist for the 5HT<sub>3</sub> receptor of serotonin, to inhibit vomit sensation after chemotherapy. The exposure of Kulchitsky cells (known as enterochromaffin cells) can lead to the production of serotonin and the stimulation of the vagus nerve result in vomiting or vomiting sensation.<sup>73</sup> Data showed that swellable MN system, containing 1.5% CaHPO<sub>4</sub> successfully released about 2.1 mg granisetron during 168 h compared to the CaHPO<sub>4</sub>-free swellable MN system.<sup>72</sup> Monitoring the systemic levels of granisetron in rats showed the highest concentrations during the early 24 h. The presence of granisetron was found during 168 h (Figure 4).

### Smart MNs

As the MN delivery system progressed, the requirement of precise control release, high agent uptake efficacy, and accurate elective cell delivery with much lower side effects become important for professional self-health administration approaches.<sup>74,75</sup> Thus, smart MNs were introduced as responsive drug delivery platforms that stimulated by exogenous, endogenous, or multi-triggers to modulate the rate, amount, and moment of transdermal drug

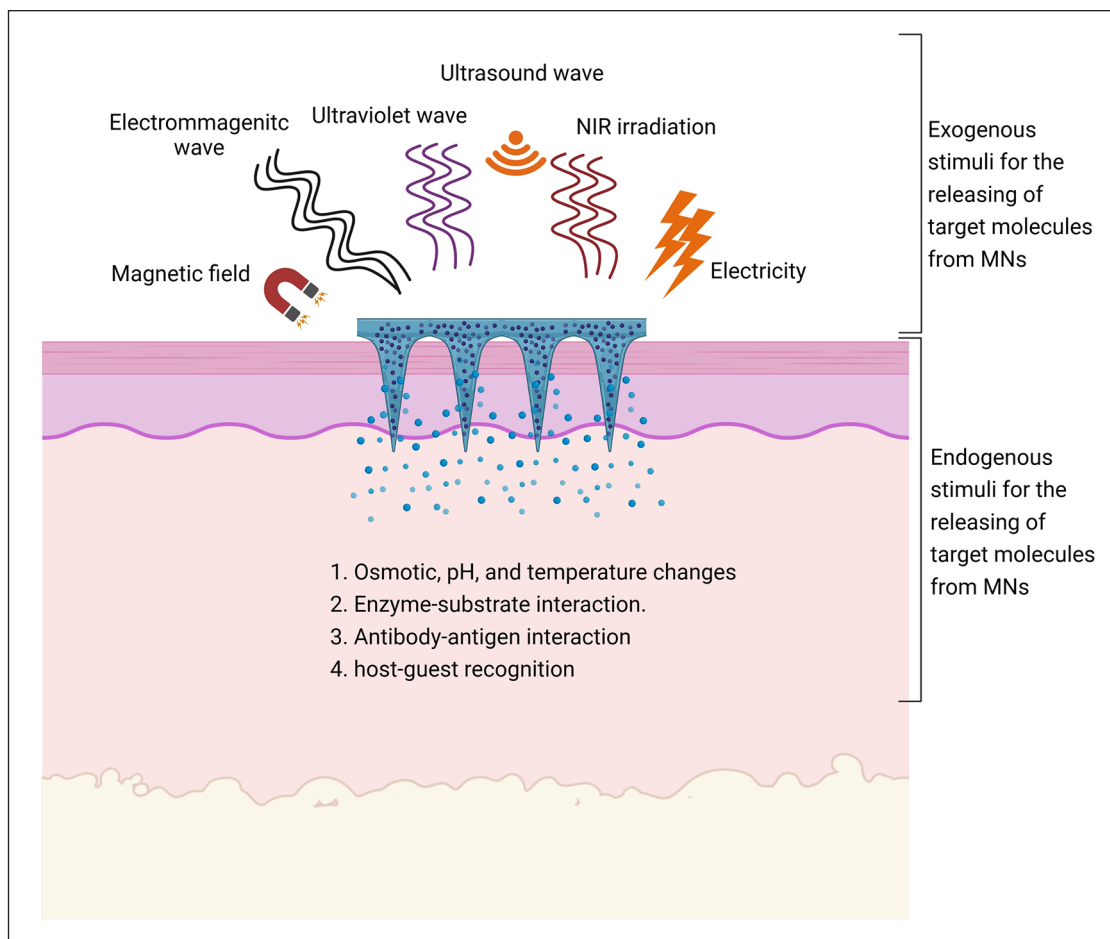


**Figure 5.** Smart MN types. The smart MN response to the environmental changes allowed controllable factor release. Smart MNs were divided into two major groups exogenous- and endogenous-based stimuli.

delivery.<sup>74</sup> In this regard, smart MNs are designed with different responsive materials. The procedure of smart MN synthesis is based on three steps that lead to MN matrix phase transition or shape-shifting (shrinkage, swelling, and leakage) and selective drug release. Steps are as follows; (I) the endogenous environmental changes in PH, or temperature, or osmotic pressure, (II) the biomolecule interaction based on enzyme-substrate interaction, or antibody-antigen interaction or host-guest recognition that is applicable to stimulate by any internal modification rates of glucose, nitric oxide, thrombin, ROS, etc., and (III) the different exogenous stimuli such as UV, NIR, electricity, magnetic field, and ultrasound, which induce dynamic bond cleavage, isomerization, reduction, or ring-opening between structural materials used in MNs (Figure 5).<sup>74–76</sup>

### Thermal and PH responsive materials

Generally, the release capability of thermoresponsive materials is dependent on reversibly hydrogen bond formation and deformation or molecular aggregation and molecular disaggregation owing to Van-Der-Waals or

hydrophobic interaction by inducing different scales of temperature.<sup>77</sup> In the case of molecular aggregation, unbalancing between hydrophilicity/hydrophobicity ratio toward temperature stimuli makes molecular disassembly and drug secretion.<sup>77</sup> Until today, variable thermo-sensitive materials with lower critical solution temperature (insoluble in high temperature) or higher critical solution temperature (soluble in high temperature) have been utilized in drug delivery.<sup>77,78</sup> For example, elastin, polypeptide, carbohydrate-based, and pluronic hydrogels, NIPAM, polyacrylic acid-co-acrylamide, PEG-based block copolymers, metal nanoparticles, carbon nanoparticles, etc. have been used to deliver drugs into the target area.<sup>77,78</sup> In an experiment, the permeability of porcine skin was successfully increased after the insertion of a solid microneedle with 600  $\mu\text{m}$  length for 48 h.<sup>79</sup> To this end, NTX-HCl was encapsulated in poloxamer 407 (P407) and applied to the skin. Data showed that the increase of ambient temperature up to 27°C caused P407 gelation and a steady release rate up to 48 h. The aqueous-loaded NTX-HCl had a higher and fast release rate.<sup>79</sup> Commensurate with these comments, any disruption on the expected local

temperature can lead to undesirable aggregation or disassembly that limits the application of thermoresponsive materials in the clinical setting.<sup>79</sup>

Due to distinct pH values in different parts of the body and cellular segments, biomaterials with the ability to respond to acidic or physiological conditions have been developed.<sup>80</sup> The pH-responsive materials are materials with acidic or alkaline groups (PKa value between 3 and 10) and ionized with electrostatic interactions following the alteration of environmental pH.<sup>77</sup> Besides, the pH-responsive materials can be modified through an oxidoreductase reaction, leading to phase shifting via pH fluctuation.<sup>81</sup> It is noteworthy to know that few pH-responsive materials are biocompatible and functional at the range of physiological. As a consequence, these features limit the choices for various experiments and conditions.<sup>77</sup> In general, block copolymers, polyamidoamine, PAA, poly L-lysine, modified derivatives of different substrates like chitosan, mesoporous silica, pH-sensitive bonds between applied material like hydrazine links, and other ionic nanostructures such as calcium phosphate, etc. have been used as pH-responsive materials for drug delivery purposes.<sup>77,80,81</sup> To study the role of pH on drug delivery, Cherng-Jyh and co-workers designed a PVP-based MN array and PLGA hallow mesosphere labeled with sodium bicarbonate ( $\text{NaHCO}_3$ ) and fluorescent probes. Upon MN degradation, the existence of a naturally acidic environment in cutaneous tissue provided an interaction probability between free protons and  $\text{NaHCO}_3$ . Thus, the production of  $\text{CO}_2$  can trigger drug extrusion.<sup>82</sup> It was suggested that about 80% of the drug is released from the hallow mesosphere supplemented with  $\text{NaHCO}_3$  in the aqueous acidic condition through 15 min.<sup>82</sup> Miao et al. provided a smart MN system consisting of an i-motif DNA/gold nano-stars/doxorubicin MN system. Doxorubicin is an efficient chemotherapy drug that triggers apoptosis by attaching to the host DNA and preventing DNA replication and RNA expression.<sup>83</sup> For this purpose, Miao et al. conjugated double-strand DNA on gold nanostars followed by insertion of aptamer on i-motif. In this system, aptamer provides a bridge to connect i-motif to DNA. However, this connection is pH sensitive. According to their data, the changes in pH and temperature values can release near 75% load doxorubicin in which cancer cells lost clonogenic capacity and malignancy.<sup>84</sup>

## Exogenous triggered MN delivery system

### Light stimulation

Among exogenous stimuli, light triggers by UV and NIR have been extensively used for photodynamic and photothermal activation.<sup>85</sup> In the case of MN stimulation by photothermal approach, the light emission (NIR and UV) excites the electrons of applied materials (mostly metal

nanoparticles, semiconductors, and carbon-based materials), and the electrons translocation to the base circuit is along with energy liberation as locally-focused heat that induces drug release by dynamic configuration in MN.<sup>85</sup> The direct UV light can also stimulate the photo-isomerization process by applying coumarins, spiropyrans, and azobenzene to increase drug delivery.<sup>74</sup> Zhang et al.<sup>86</sup> designed a separable PVA-gelatin methacryloyl- (Gel-MA) loaded with black phosphorous dots (as photothermal conversion molecule) and hemoglobin immersed in oxygen solution for diabetic cutaneous wounds therapy. An impaired wound healing in diabetic patients occurs because of prolonged hyperglycemia, production of inflammatory cytokine, and ROS for a longer period.<sup>87,88</sup> Additionally, it is thought that every hemoglobin molecule can carry four oxygen molecules and immersion in oxygen solution causes more oxygen uptake. To alleviate the hypoxic condition, these patches were attached to diabetic rat cutaneous wounds and exposed to NIR. Upon NIR irradiation, oxygen molecules were released into the skin by increasing the temperature. This strategy can help us to impede long-term severe hypoxia and increase the possibility of chronic wounds treatment.<sup>86</sup> NIR stimuli are popular due to their tissue permeability capacity and are mostly absorbed by tissues. Therefore, it is necessary to consider safety issues during the application. The photodynamic process is often promoted using energetic UV light.<sup>85</sup> During the photodynamic process, the photosensitizer molecules are delivered by MNs to produce ROS following the exposure to UV irradiation, leading to tumoricidal effects.<sup>89</sup> In these circumstances, the photosensitizer liberation is controlled by the degradation rate of the MN matrix. For instance, ALA is a photosensitizer molecule converting to PPIX in the mitochondria after NIR stimulation. Although ALA showed promising results in the potential of ROS production, the traditional transdermal delivery was challenging due to the natural hydrophilic properties of ALA.<sup>90</sup> Photodynamic responsive molecules face some limitations in *in vivo* conditions such as low stability rate and the need to use high doses to achieve promising results.<sup>89</sup> In this regard, Zhao et al. developed local delivery based on ALA to overcome former limitations. They used tip-loaded fast dissolvable hyaluronic acid MNs with a depth of about 200  $\mu\text{m}$  encapsulated ALA for subcutaneous tumor therapy in a mouse model. According to data, the dissolving MNs delivered a large amount of ALA during the early 10 min. This system had perfect progress compared to previous ALA-coated MN delivery systems. Data also showed significant tumor inhibition in ALA-loaded hyaluronic acid MNs compared to direct injection of ALA (97% vs 66%).<sup>90</sup>

### Magnetic stimulation

The magnetic particles that are placed inside the soft or thermo-sensitive materials could be activated by the MF

remotely, providing a safe delivery platform without tissue penetration despite the light stimulated delivery technique.<sup>75</sup> The major action mechanism of magneto-responsive materials is the dynamic bond deformation and heat production by magnetic particles within the MN construction. Moreover, the released agents could be directed to the desired site in the presence of magnetic forces.<sup>75</sup> However, the minority of responsive materials to magnetic stimulation, production of toxic derivatives due to magnetic particle degradation, the possibility of severe local heat generation, and high-cost instrument necessity have limited bulk application of magnetic stimulated MNs for transdermal drug delivery.<sup>91</sup> To examine the MN delivery system triggered via a magnetic field, Fang et al. developed a PVA-mesoporous iron oxide nanoraspberry based MNs loaded with Minoxidil. The size of MNs reached 600–300  $\mu\text{m}$  in height and round base diameter, respectively.<sup>92</sup> Minoxidil is commonly used to improve hair growth by vasodilation effects, induction of cellular proliferation, growth factor production.<sup>92,93</sup> Upon using MF, the viability of rabbit synovocytes, HIG-82, was reduced because of local heat generation, and the toxicity of the iron oxide nanoparticles. Loading Minoxidil in PVA-mesoporous iron oxide nanoraspberry based MNs increased hair density in alopecia areas after 7 days. It was suggested that the further release of Minoxidil after MF stimulation increased local blood flow after regulation of K channels, relaxation of vascular smooth muscle, production of VEGF, and PEG<sub>2</sub>.<sup>94</sup>

### Ultrasound stimulation

As aforementioned, ultrasound triggering through the sonophoresis process enhances skin permeability via both thermal and non-thermal approaches.<sup>75</sup> During ultrasound emission, the created microbubbles were moderately wobbled which plays a critical role in the skin permeability enhancement.<sup>21</sup> Additionally, the stable cavitation promoted by stably teetering microbubbles occurs through low-frequency ultrasound waves.<sup>21</sup> Given the high-frequency ultrasound waves, the microbubbles were teetered vigorously leading to microbubble destruction through inertial cavitation and proximal cellular death. However, inertial and stable cavitation is also important for drug delivery applicants.<sup>21</sup> Ideally, the application of higher amounts with smaller-sized microbubbles with 6–11 second stability are effective agents to increase the efficacy of transdermal drug delivery.<sup>95</sup> Additionally, the biodegradation of polymers could be controlled by ultrasound treatments.<sup>75</sup> However, long-term ultrasound treatment and the production of microbubbles with temporary and lower stability are problematic.<sup>91</sup> In this regard, Zandi et al.<sup>95</sup> fabricated electrochemical-based MNs coated with ZnO nanowires to promote the uptake efficacy of anti-cancer drug PTX by performing an electrolysis reaction through interstitial fluid. Based on recent knowledge, the multiplication of cancer cells was limited through

inhibiting AKT/MAPK signaling pathway and stimulating P53, which arrests cell cycle via activating P21 and cyclin B1, by treating cells with PTX.<sup>96</sup> Additionally, PTX-induced ROS production can lead to up-regulation of Bax, Caspases 3 and 9, and apoptotic cell death. The insertion of MNs and application of  $-2\text{V}$  voltage pulses led to the production of smaller and higher amounts of microbubbles.<sup>95</sup> In vivo findings revealed about 82% tumor suppression in tumorized mice model of breast cancer exposed to ultrasound plus MN treatment within 10 days. The induction of P53, suppression of nuclear Ki-67 coincided with cell cycle arrest were touted as main oncostatic effects in these mice.

### Electric stimulation

Iontophoresis and electroporation are other transdermal drug delivery approaches that are based on electrical stimulation.<sup>97</sup> In comparison to iontophoresis, electroporation implies a higher voltage of approximately 100 V to improve skin permeability whilst in the iontophoresis process, fewer values (about 10 V) of electrical stimulation are used to promote redox reaction and ionized agents transportation between electrodes and the skin.<sup>97</sup> During iontophoresis, two electrodes namely anode and cathode were positioned in the interstitial fluid of the skin. By applying the reference voltage, positive ions were conveyed to the skin at the anode and vice versa.<sup>98</sup> Previous studies have used a large variety of MN-based electrochemical devices by conductive materials such as polypyrrole and nanowires toward biosensing and delivery approaches.<sup>99</sup> Iontophoresis provides an accurate controllability drug release system. Of note, insufficient macromolecules delivery and sustainable reaction at the site of insertion limit iontophoresis.<sup>100</sup> To address these issues, Yang et al.<sup>100</sup> fabricated a smartphone-powered iontophoresis-MNs for the electrically controlled release of insulin. The designed iontophoresis circuit consisted of an MN patch (as the anode), Ag/AgCl electrode as the cathode, and smartphone as the resource of energy. Additionally, the fabricated MN patch was equipped with a tape, a gasket (prevent drug leakage), an electrode with PMMA film, and a medical sponge consisting of insulin encapsulated positive vesicles.<sup>100</sup> Data showed that the application of iontophoresis alone lacked effective insulin delivery capacity in type 1 diabetic SD rats while MN patch with positively encapsulated insulin can stabilize glucose level within 5.7 h and this value was 2.7-fold higher than the injection group.<sup>100</sup>

### Endogenous stimulation of MN delivery system

Notably, the closed-loop MN delivery systems eliminated the additive sampling necessity before injection. However, non-responsive MN delivery systems and traditional hypodermic needles called open-loop delivery systems impede probable erroneous feedback, biofouling, and further immunogenicity.<sup>101</sup> Nonetheless, the real-time monitoring possibility and

the accurate controllability of drug release through stimuli-responsive MN delivery systems are undeniable.<sup>101</sup> Owing to highlight the importance of settable drug replenishment via closed-loop MN delivery systems, Zhang et al.<sup>102</sup> designed a thrombin responsive hyaluronic acid-based MN array to deliver heparin timely and modulate both blood clotting and unwanted bleeding. In this regard, they integrated a thrombin cleavable peptide in the MN matrix which allowed heparin replenishment in the existence of thrombin. The designed MN released heparin sustainably within 12h in response to different concentrations of thrombin.<sup>102</sup> As well, the heparin was released wobbly by positioning in existence or absence of thrombin every 15min. Data showed increased PT and PTT duration in a mouse model, indicating a postponing in blood clotting after insertion of MN. Of note, direct injection of the heparin delayed PT and PTT duration more than that of designed MNs.<sup>102</sup> However, the experimental mice with directly injected heparin or heparin encapsulated MNs were survived for only 1h. It seems the sudden release of heparin by non-responsive MNs is responsible for the mortality of mice.<sup>102</sup> Hence, mice treated with the thrombin responsive MNs were survived for 12h. Unwanted subcutaneous bleeding can be indicated due to local accumulation of heparin after insertion of conventional MN delivery system whereas the designed responsive MN only showed small-sized lesions.<sup>102</sup> McAlister et al. developed PVA-based MNs to deliver antibiotics that are used orally. This system supports efficient antibiotic delivery because of less antibiotic degradation compared to the oral route. It seems that the release of the drug is stimulated in response to endogenous osmotic pressure. After the soaking of MNs within the interstitial fluid, the needles are swelled and osmotic pressure provides the necessary force to push the antibiotic out of the needles.<sup>70</sup> As well, the drug delivery rate could be controlled due to interaction between ROS productions and ROS responsive MNs consisted of Thioether, Arylboronic ester, Selenide, or telluride containing polymers.<sup>89,103</sup> To examine this concept, the polymeric vesicles concluded (PEG)/PPBA, as glucose sensitive material, PPBEM, as H<sub>2</sub>O<sub>2</sub>-sensitive material, insulin, and GOx have been encapsulated in PVP/PVA-based MNs. The increase of glucose can alter the electrostatic equilibrium of polymeric vesicles through glucose oxidase activation. Subsequently, the production of H<sub>2</sub>O<sub>2</sub> via glucose oxidase activity is associated with the whole polymeric vesicle's disassembly and insulin leakage into the *in vivo* site (Figure 6). The directly injected insulin reduced the glucose level in 2h and rehabilitated after 10h while the designed MN insulin delivery system gradually diminished the glucose level in 4h returning to the initial levels during 10h.<sup>104</sup>

### Drug loading and efficiency

According to numerous experiments, drug or therapeutic agents can be incorporated onto or into the MNs using different modalities. The development of the small-scale device with varied drug quantities is one of the main challenges that

should be clinically considered.<sup>105</sup> Considering the high loading capacity of the MN system, fewer drug contents are needed for effective treatment. Drug loading is done in the MN system using layer-by-layer, spray, or coating approaches.<sup>106,107</sup> Drug-loaded MNs can be fabricated using a modified casting process in which the drug was mixed with the dialyzed biomaterials like chitosan solution and applied onto the PDMS mold as the first layer, and the centrifugation process was used to fill the mold cavities. To assess the releasing efficiency, the stability and release of encapsulated bovine serum albumin were examined from chitosan-based MNs.<sup>108</sup> As previously mentioned, the loading capacity of the MN system is high. In MNs made of methacrylate hyaluronic acid (MeHA), a wide range of small hydrophilic, hydrophobic, and therapeutic biomacromolecules can be loaded with the subsequent release. A high swelling rate permits efficient and effective drug loading (10µg/cm<sup>2</sup>). For instance, data have shown that over 80% of fluorescein, FITC-Dextran, and >50% of Doxorubicin are released from the MNs within early 30min. It was also estimated that >95% of the Dox was released after 72h.<sup>71</sup> Despite these advantages, MNPs should be stored under appropriate temperatures and humidity allowing drug activity and release. In another study, trehalose-stabilized influenza vaccines coated onto microneedles have been used extensively. Of note, vaccine activity is blunted over time along with sugar crystallization.<sup>109</sup> The nature and activity of loading molecules should be also considered. For example, dissolving MNs can maintain human growth hormone activity over 15 months at room temperature in the carboxymethylcellulose/trehalose system.<sup>11</sup> Additionally, multi-layered polyvinyl alcohol (PVA) dissolving MNs have been employed as effective insulin delivery systems. It was estimated that more than 99.4% of loaded insulin remained stable in the MNs at room temperature for 20 days.<sup>110</sup> Parathyroid hormone formulated in sucrose, EDTA, HCl, and polysorbate 20 exhibited longer activity coated MNs for 2 years without refrigeration. The application of sterilization methods such as gamma irradiation before depository is associated with reduced drug stability.<sup>111</sup> In different phase II clinical trials, parathyroid hormone-loaded MN systems were used for the therapy of osteoporosis. These MNs can be self-administered by patients and factor enters immediately into the bloodstream. As a correlate, MNs delivery is associated with improved clinical effects of increased bone mass density.<sup>112</sup>

### Application of MNs in diabetic condition

Diabetes is a metabolic disorder caused by insulin deficiency or cellular receptor failure resisting secreted insulin.<sup>113</sup> Untreated diabetic conditions can cause subsequent irreversible conditions like nephropathy, neuropathy, cardiovascular disorders, retinopathy, and mental disorders.<sup>114-117</sup> Currently, the patients typically use daily subcutaneous insulin injections to overcome complications associated

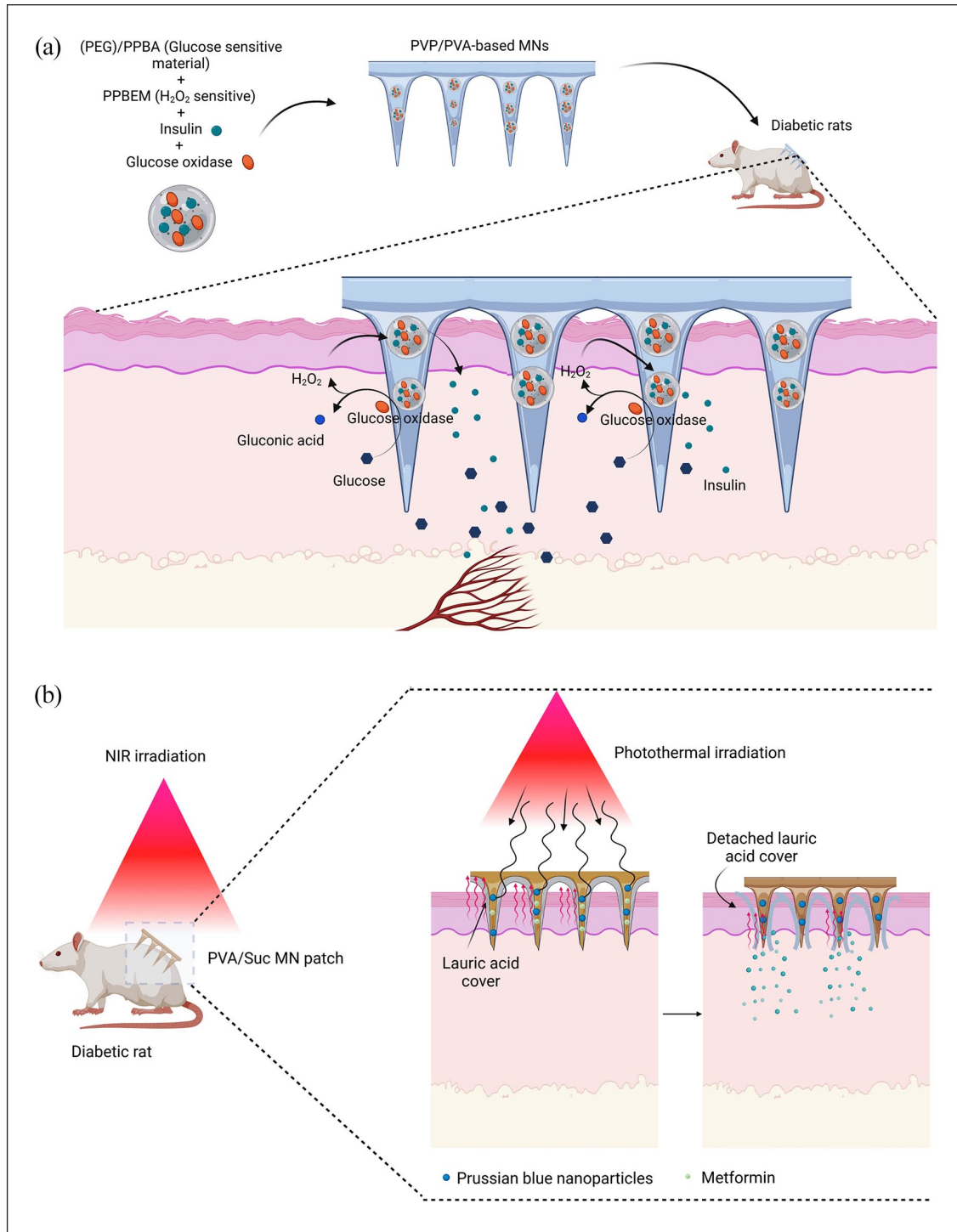


**Figure 6.** (a) Application of PVP/PVA-based MN containing polymeric vesicles consisted of PPBEM, as  $H_2O_2$ -sensitive material, (PEG)/PPBA, as glucose-sensitive material for transdermal delivery of insulin in a rat model of diabetes. Local accumulation of glucose activates glucose oxidase (GOx), leading to the production of  $H_2O_2$  and gluconic acid. In the next step, the exposure of PPBEM to  $H_2O_2$  supports the release of loaded insulin into the systemic circulation. (b) NIR emission elicits Prussian blue nanoparticles that transform light to heat. After heat production, the coated lauric acid was dissolved, causing metformin relinquishment.

with insufficient insulin production.<sup>118</sup> The recent studies also introduced analog peptides of glucagon hormone and its receptor to modulate glucose rate.<sup>119,120</sup> Although, the

subcutaneous insulin injection is a fast way to control hyperglycemia, the infection possibility, painful multi-daily injection, post-disposal of the syringe, and constant glucose

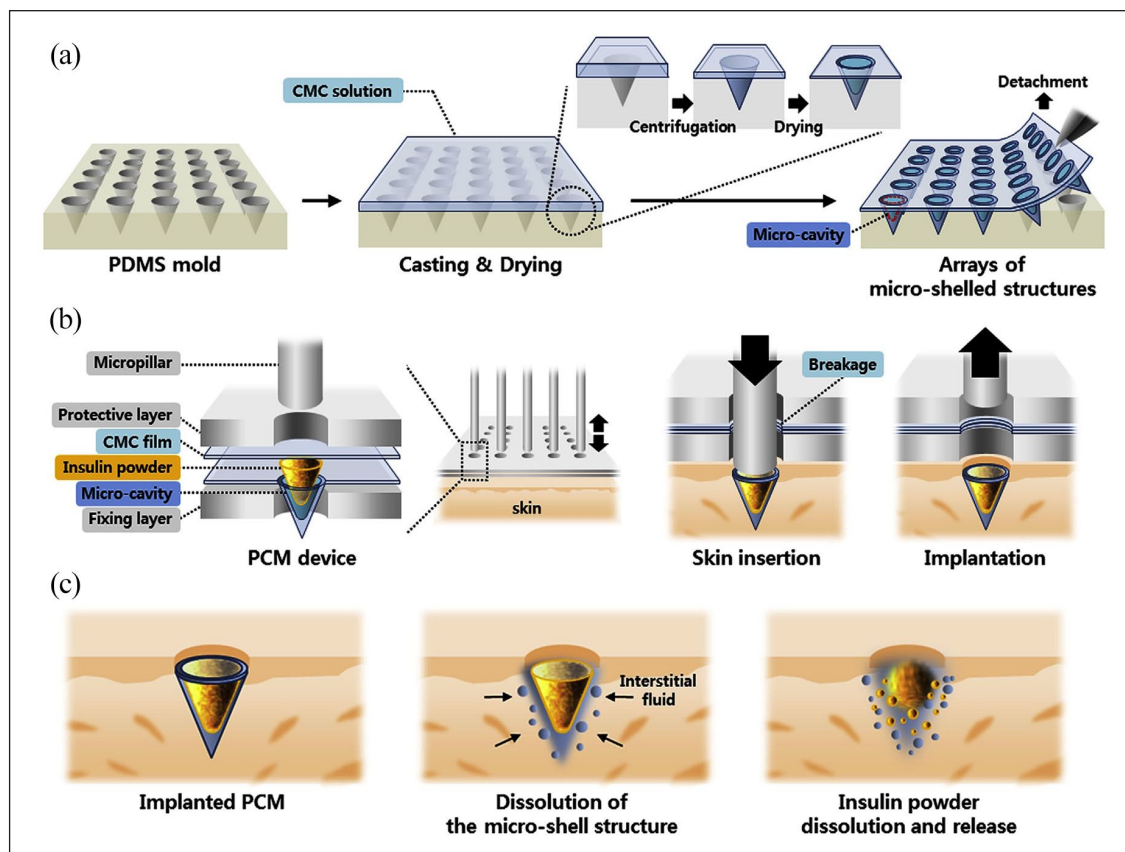


**Figure 7.** Representative illustration related to fabrication and application of insulin-loaded powder-carrying microneedle using PDMS mold, and CMC solution (a). Dissolving MNs possess empty cavities. Upon detachment of MNs from the mold, insulin powder was loaded into the micro-cavities and coated with CMC film (b). The insertion of these MNs into the cutaneous layer leads to the breakage of the CMC layer at the base of patches. The retraction contributes to the remaining of MNs within the cutaneous layer (c). These MNs adsorb the interstitial fluid thus insulin is released accordingly. Source: Adapted with permission; Copyright 2020; Biomaterials.<sup>123</sup>

monitoring have limited the efficacy of insulin delivery through the subcutaneous route. To overcome these limitations, the nasal, pulmonary or inhaling, buccal, oral, rectal, ocular, vaginal, intraperitoneal, and transdermal routes have been implicated for insulin delivery.<sup>121</sup> Nonetheless, the alternative routes are restricted owing to the low bioavailability and possible enzymatic degradation, slow and low local absorption, local insulin accumulation, and subsequent inflammations.<sup>121</sup> In this regard, recent MN technology has been developed to improve insulin permeability, stability, and bioavailability through alternative routes. However, the bioavailability of the peptide would be affected if pH or temperature modified severely while MN fabrication or post-product retention process.<sup>122</sup> Besides, peptides activity could be biased via organic solvent persistence that is mostly utilized while MN fabrication.<sup>122</sup> To address this issue, Kim et al. constructed an open-loop MN delivery system that resembled microcavities. Respectively, they cast insulin powder into microcavities built by CMC to impede insulin degradation and dose dilution through combining with supportive polymer solution in conventional dissolving MN

(Figure 7).<sup>123</sup> According to their study, 10% of CMC exhibited proper penetration and high capacity for insulin loading. The fabricated MN improved insulin stability about 5% better than conventional dissolving MN within 8 weeks at 25°C. Nonetheless, delayed insulin distribution has been shown by powder-loaded MN on the in vitro release profile.<sup>123</sup> In vivo results showed that the serum content of glucose was decreased rapidly via subcutaneous injection whereas the glucose reduction was delayed by both dissolving and subsequently powder-loaded MNs. Moreover, insulin was absorbed through dissolving and powder-loaded MN only about 60% while the whole injected insulin had been absorbed subcutaneously.<sup>123</sup> Calling attention, the water loss caused by trans-epidermal was retrieved to standard points until 12 h after MN insertion.<sup>123</sup>

Progressively, the recent studies attempted to overcome the limitations of an open-loop MN delivery system like severe hypoglycemia resulted in high dose insulin delivery.<sup>84,124</sup> To this end, the closed-loop MN delivery systems have been developed to kinetically modulate hyperglycemia upon 3 policies including (1) utilizing glucose-responsive

materials that react as pancreatic  $\beta$ -cells alternatives, (2) conveying healthy  $\beta$ -cells along with glucose sense amplifiers, or delivering immunogenic antigen to the damaged target, and (3) implicating exogenous stimuli-responsive material.<sup>101,125</sup> Among them, the closed-loop glucose-responsive materials are based on (1) GOx systems that could optimize with pH-, hypoxia-, and  $H_2O_2$ -responsive matrix, (2) Competition-based systems is based on the reversible affinity of Concanavalin A (Con A) binding to D-glucose and polysaccharides, and (3) Reversible bond formation between Phenylboronic acid (PBA) and glucose.<sup>101,126</sup> Notably, Con A and PBA exhibited less biocompatibility and volatile affinity to glucose.<sup>127,128</sup> Especially, PBA interacts with glucose in high pH environment better than physiological pH.<sup>127</sup> However, the use of GOx also has been limited by the risk of ROS production and enzymatic degradation within manufacturing.<sup>127</sup> In MNs based on GOx, glucose is converted to gluconoidacid that decreases local pH. The procedure continues with the production of  $H_2O_2$  as a further byproduct in the presence of oxygen and a high concentration of glucose.<sup>126</sup> Considering these advantages, pH-responsive and/or ROS responsive materials were implicated to fabricate GOx-based MNs for facilitating insulin release.<sup>126</sup> However, the speed of response to glucose level modifications could be interrupted via the local pH reduction.<sup>128</sup> To solve this issue, Yu et al.<sup>128</sup> fabricated HA-based MNs encapsulated vesicles that involved HA, hydrophobic NI, insulin, and GOx. In this MN system, NI is reduced to hydrophilic 2-aminoimidazoles after production of NADPH induced by GOx redox activity and oxygen expending mimics hypoxia-like condition.<sup>128</sup> Moreover, the HA backbone of the MN patch improved mechanical strength to suitably penetrate the skin and inhibited sudden extrusion of HA-based vesicles. Based on *in vivo* findings, the glucose level was rapidly diminished and started to increase gradually after 4 h. In an MN system without GOx, no significant glucose reduction was achieved.<sup>128</sup> As well, MN-loaded insulin alone decreased rapidly the level of glucose. However, the percentage of hypoglycemic risk had been significantly high compared to MN loaded HA based vesicles with or without GOx.<sup>128</sup> According to these data, applying MN-loaded HA-based vesicles with GOx secondly after 1 h led to lack of hypoglycemic condition, suggesting prolonged normal rate of glucose for another 3 h in *in vivo* condition.<sup>128</sup>

In another study, a rapidly glucose-responsive porous-coated MN delivery system was designed via a dip-coating process to solve delayed glucose response via GOx-based systems. The porous polymer consisted of glucose oxidase, sodium bicarbonate, a pH-responsive component, and insulin.<sup>129</sup> Briefly, the insulin released through glucose and glucose oxidase interaction made protons and decrease pH. The accumulation of  $CO_2$  causes insulin extrusion and a significant reduction in plasma sugar.<sup>129</sup> Based on the *in vitro* release profile, the pulsatile insulin release was seen

under the exposure of various concentrations of glucose (Figure 7(a)).<sup>129</sup> As well, a high concentration of glucose facilitated faster insulin release proportionally associated with high GOx activity and more  $CO_2$  production. The designed MN released 53% of insulin 1 h after hyperglycemia in *in vivo* condition and the concentration of blood glucose decreased below 200 mg/dl within 3 h without the risk of hypoglycemia. Besides, this normal rate of glucose was maintained about 10 h after applying designed MNs.<sup>129</sup>

Recently, a plethora of data has shown the critical role of regulatory T lymphocyte activity in the suppression of autoimmune-mediated diabetes.<sup>130</sup> In this regard, Singh et al.<sup>130</sup> utilized a hollow MN delivery system (MicronJet600™) to inject subcutaneously gold nanoparticles conjugated with less-soluble immunogenic peptides. Based on the experiment, the diabetogenic regulatory T-cells were intravenously injected and peptides were subsequently delivered via MN. Data indicated an increased T lymphocyte proliferation in distant lymphoid organs like pancreatic lymphoid nodes.<sup>130</sup> The combination of peptides and nanoparticles promoted T cell expansion in remote areas like lymphoid nodes, draining lymphoid, spleen, and pancreatic lymphoid nodes after 48 h while T cell proliferation via peptide in the absence of gold nanoparticles was only seen in draining lymphoid nodes after 72 h.<sup>130</sup> Moreover, these values were insignificantly modified through the MN delivery system when compared to subcutaneous injection. Additionally, the existence of a higher affinity of water-soluble peptides to T lymphocytes leads to cellular proliferation and significant distribution related to less-soluble peptides. Notably, the combination of water-soluble peptides and nanoparticles reduced the functionality of water-soluble peptides.<sup>130</sup> This strategy decreased the expression of IFN- $\gamma$  in the auxiliary lymphoid nodes after 3 days.<sup>130</sup> In CCR7<sup>-/-</sup> mice, the immune response is blunted due to the lack of CCR7 and diminished dendritic cell homing in lymphoid nodes. The combination of gold nanoparticles plus peptide and peptide alone were distributed to lymphoid nodes through dermal dendritic cell migration and proliferation.<sup>130</sup>

In comparison between endogenous and exogenous delivery approaches, exogenous stimuli are more flexible to personalize the designed MN device because of applying external stimulation which is adjustable in severity and duration.<sup>76</sup> To develop an example of exogenous MN delivery, a separable PVA/sucrose-based MN coated lauric acid included PB-NPS, a photothermal conversion molecule, and metformin drug was used in diabetic conditions (Figure 6).<sup>131</sup> Metformin is known for its AMPK signaling pathways provocation that facilitates hepatic gluconeogenesis inhibition in diabetic patients.<sup>132</sup> Upon exposure to NIR, PB NPs convert light to heat, and lauric acid melts at 44°C allowing metformin release.<sup>131</sup> Precaution should be taken that high local temperature or slightly increased local temperature leads to tissue damages for a high duration. In this regard, a low concentration of PB NPs (about 0.1% wt) was selected

to treat with NIR for 90s every 2h.<sup>131</sup> Based on data, the glucose level diminished after 6h and reached the same levels obtained via direct insulin injection. However, the normoglycemia was stable more (about 1h) in the MN system compared to the direct insulin injection.<sup>131</sup> The biocompatibility and low immunogenicity of designed external stimuli MN should also be considered. There are few reports demonstrating tissue lesions in the heart, liver, spleen, kidneys, and lungs examined by histopathological examination. The increase of local interleukin-1 beta (IL-1 $\alpha$ ) has been indicated in cutaneous tissue using immunofluorescence imaging.<sup>131</sup> In another study, Di et al.<sup>133</sup> developed insulin-loaded PLGA nanoparticles encapsulated in chitosan microgels. The designed MN system was stimulated via ultrasound waves to improve microbubble stability that leads to sustainable insulin release.<sup>133</sup> Owing to eliminate erroneous side effects of ultrasound treatment, the input voltage, pulse duration, and treatment elongation should be carefully arranged. In this regard, 400mV was used for every 20 $\mu$ s within 30s once a day until the 10th day.<sup>133</sup> The use of ultrasound stimulation led to the burst release of insulin for a while then the passive replenishment of insulin has been observed in the absence of ultrasound emission.<sup>133</sup> Based on in vivo results, the glucose rate was rapidly decreased about 10min after every treatment.<sup>133</sup> Normoglycemia was reported within the first 3 days after MN application. Under these circumstances, the glucose levels became within normal ranges even after the sixth treatment, indicating MNs as successful sustainable insulin delivery devices (Table 1).<sup>133</sup>

### Immunotherapy using MNs

Vaccination is a traditional approach for immunization via the controlled presentation of single antigens or collection of antigens to the immune system cellular subsets. This strategy induces antigen-specific immunization against viral, bacterial, or parasitical infectious diseases, and non-infectious diseases such as cancer and atherosclerosis.<sup>150,151</sup> Moreover, recent studies have developed novel vaccination approaches to regulate and control antigen-specific immune system activity to prohibit the occurrence of autoimmune diseases like Alzheimer's disease, diabetes, multiple sclerosis, auto-immune-based inflammatory diseases, etc.<sup>150</sup> The most important goal of vaccination is to trigger long-term and active antigen-specific immunization by provoking the adaptive immune system leading to antigen-specific T lymphocyte cell activation, B lymphocyte recruitment, and generation of memory cells.<sup>150,151</sup>

### Vaccine designing and MNs

For designing an effective vaccine, various parameters like the type of antigen, adjuvant, antigen carrier, manufacturing process, and the delivery system should be considered.<sup>152</sup> Antigens are distinct biomolecules with specific

epitopes eliciting the immune system response. For instance, attenuated or inactivated viruses, a viral subunit, recombinant proteins, peptides, and nucleic acids are popular antigens that have been used to design vaccines against viral infections.<sup>152-155</sup> In cancer immunotherapy, different tumor-associated antigens were isolated from the tumor mass. These antigens are commonly proteins released from cancer cells more than that of normal cells. Of these proteins, HERVs are familiar with the development of vaccination.<sup>156</sup> Interestingly, the engineered antigens could be chemically linked with adjuvants to improve immunogenicity during nucleic acid-based and protein-based vaccinations.<sup>152</sup> To elicit stability and accurate targeting capability of antigens toward APCs, the antigens also could be conveyed via viral and non-viral carriers.

In recent decades, hypodermic injection, implantation, and MN delivery system have been touted as the most convenient ways of vaccination.<sup>152</sup> Of note, the advantage of MN technology is the painless, self-administration compared to subcutaneous implantation. The sophisticated manufacturing process, stability of antigen, and post-production concerns about antigen activity have limited the extensive application of MNs in the clinical setting.<sup>152</sup> Of note, hollow MN, dissolving MN, micron jet, and Soluvia device are the most general MN-based delivery tools for vaccination against tumors.

### Signaling pathways associated with transdermal delivery of antigens via MNs

Upon introduction of specific immunogens (antigens or epitopes) to the target sites, the immunization is initiated by the recruitment and activation of APCs in the early stages. Like other tissues, cutaneous APCs have been thought to be activated following the introduction of antigens via MNs. Of cutaneous APCs, Langerhans cells (CD1a/CD207) are located at the epidermal layer. In addition, two subsets of dermal dendritic cells (CD1c<sup>+</sup> and CD141<sup>+</sup>), dermal monocyte-derived macrophages (CD14<sup>+</sup>), FXIIIa<sup>+</sup> macrophages, and B lymphocytes are essential in the procedure immunization occurred via the transdermal route. It was suggested that all these cell types are recruited to the site of injection following skin sensitization.<sup>150,153,157,158</sup> Each kind of APC possesses distinct activation potential, migration rate, and antigens presenting capacity after immunization, leading to prime adaptive immunity. Fukunaga et al. acclaimed that dermal dendritic cells migrate faster and in large numbers to the draining lymph nodes for presenting antigens to T lymphocytes compared to Langerhans cells.<sup>159,160</sup> In general, APCs are activated using three strategies as follows; (I) Production of endogenous pro-inflammatory cytokines (e.g. TNF- $\alpha$ , IL1- $\beta$ , -18, -6, and IFN- $\alpha$ ) via activated inflammatory cells, keratinocytes or APCs; (II) Release of endogenous molecules namely DAMP that

**Table 1.** Different MN types and applications.

Drug Name	MN type	Fabrication method	Material	Mechanism of action	Therapeutic applicants	Ref
Lysozyme enzyme	Dissolving MN	Micromolding	Polyvinylpyrrolidone, hyaluronic acid, and poly(lactic-co-glycolic acid)	Breaking glycosidic bond in peptidoglycans	Antibiotic for dermal use	Panda et al. <sup>134</sup>
Resveratrol	Dissolving MN	Micromolding	Eudragit/PVP-K90/Resveratrol	Inhibiting TGFβ/SMAD pathway	Cosmetic, skin cancer, cardiovascular disease	Aung et al. <sup>135</sup>
Nicotine	Dissolving MN	Micromolding	Polyvinylpyrrolidone/Nicotine	PI3K-Akt signaling pathway	Smoking addiction	Panda et al. <sup>136</sup>
Silver nanoparticle	Dissolving MN	Micromolding	Silver nanoparticles were encapsulated in Polycaprolactone/Chitosan as microparticles surrounded by Polyvinylpyrrolidone/Polyvinyl alcohol	Inhibition PI3K/AKT signaling pathway by ROS production, Interruption cell wall	Infectious chronic wound	Permana et al. <sup>137</sup>
Dexamethasone	Dissolving MN	Micromolding	Hyaluronic acid and Collagen were encapsulated inside poly(lactic-co-glycolic acid) and loaded with Dexamethasone	Inhibition of NLRP3 and IL-1β production	Inflammatory skin disorders	Wan et al. <sup>138</sup>
Rosi	Smart/Dissolving MN	Micromolding	Polyvinyl alcohol/Melanin/Rosi	Inhibition of peroxisome proliferator-activated receptor (PPAR)	Obesity	Peng et al. <sup>139</sup>
Capsaicin	Dissolving MN	Micromolding	Capsaicin was encapsulated in α-Lacnano micelles/Hyaluronic acid/Polyvinyl alcohol	Reduction of PPARγ, C/EBPα Promotion of AMPK signaling pathway	Obesity	Bao et al. <sup>140</sup>
Lix	Dissolving MN	Micromolding	PVPK29/32/Lix	cAMP/PKA, PIP3/PKC, and PI3K/AKT signaling pathways	Diabetes	Zhu et al. <sup>141</sup>
Glucagon	Swellable MN	Micromolding	Methacrylated hyaluronic acid/Glucagon loaded in microgels consist of zwitterionic sulfobetaine (SB), 4-acrylamide-3-fluorophenylboronic acid (AFBA), and cationic carboxybetaine (CB)	cAMP/PKA and PIP3/PKC signaling pathways	Diabetes	GhavamiNejad et al. <sup>141</sup>
Viral subunit	Dissolving MN	Micromolding	PVP/Lyophilized monovalent subunit: influenza vaccine (A/Brisbane/10/10 (H1N1))	Biodegradation	Vaccination	Kim et al. <sup>142</sup>
mRNA	Dissolving MN	Micromolding	PVP/Naked luciferase mRNA	Biodegradation	Transfection	Koh et al. <sup>143</sup>
Viral vector loaded antigen-adjuvant	Dissolving MN	Micromolding	Carboxymethyl cellulose/trehalose loaded ovalbumin mRNA with Poly(l-C) (TLR3 against)	Biodegradation	Vaccination/Transfection	Erdos et al. <sup>144</sup>
Non-viral vector loaded DNA	Dissolving MN	Micromolding	PVA/PVP encapsulated poly lactic-co-glycolic acid—poly-L-lysine/poly-γ-glutamic acid (PLGA-PLL/γPGA) nanoparticles/Ebo DNA	Biodegradation	Transfection	Yang et al. <sup>145</sup>
Viral subunit coadjuvant	Dissolving MN	Micromolding	Sucrose/gelatin encapsulated P47/CpG oligonucleotide	Biodegradation	Transfection	Yenkoidiok-Douti et al. <sup>146</sup>
Viral subunit coadjuvant	Dissolving MN	Micromolding	PVA/sucrose loaded H1N1 co cGMP/saponin	Biodegradation	Transfection	Vassilieva et al. <sup>147</sup>
DNA encoded bacteria toxin	Dissolving MN	Micromolding	Hyaluronic acid loaded pVAX1 ( plasmid DNA) encoded Ag85B of Mycobacterium tuberculosis	Biodegradation	Transfection	Yan et al. <sup>148</sup>
Non-viral vector loaded DNA	Dissolving MN	Micromolding	PVA loaded RALA/pPSCA (Prostate Stem Cell Antigen)	Biodegradation	Transfection	Cole et al. <sup>149</sup>

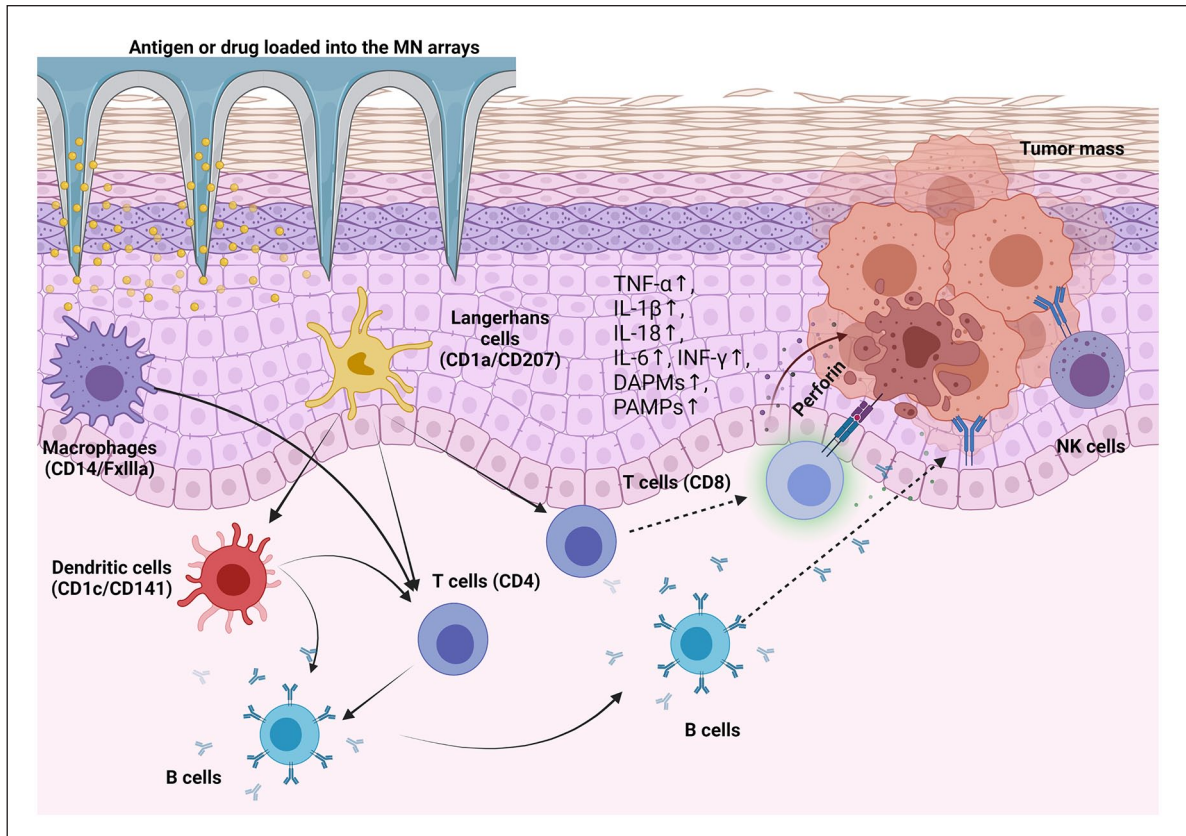


**Figure 8.** Schematic of antigen-specific immunogenicity by MN delivery system. MN arrays can deliver antigen/or therapeutic agents into the dermal layers. In the next steps, antigens are processed by local APCs, leading to activation of T lymphocytes (CD8, CD4<sup>+</sup> lymphocytes) and B cells. In addition to the production of numerous cytokines, immune cells like NK cells and CD8 lymphocytes can directly invade the tumor cells.

is produced in injured cells after the arrival of exogenous pathogen and replication inside the cells. DAMPs are composed of DNA, RNA, cellular proteins, etc.<sup>161–163</sup> and (III) Production of the PAMP and adsorption of these components via phagocytosis, pinocytosis, and endocytosis by different cellular receptors such as TLR, C-type lectin receptors, etc.<sup>161,162</sup>

### APCs activation after MNs immunization

Following the application of antigen-loaded MNs, the cutaneous tissue is immunized physicochemically and different pro-inflammatory cytokines (e.g. TNF- $\alpha$ , IL1 $\beta$ , -18, -6, and IFN- $\alpha$ ) are released keratinocytes or other resident cells (Figure 8).<sup>162,163</sup> In general, these cytokines activate several cellular signaling pathways like NF- $\kappa$ B, MAPK, and JAK/STAT, accelerating APCs maturation. In later steps, the activated APCs migrate into the parenchyma of draining lymph nodes, and further present antigens to naive T lymphocytes.<sup>163–165</sup> Typically, the activated APCs have less phagocytosis ability compared to their inactive counterparts. Of note, bioactivities such as antigen

processing and presenting, migration, and induction of lymphocyte differentiation are increased in APCs through activation.<sup>162</sup> The activated APCs obtain different cellular markers like CCR7, antigen-presenting markers that is MHC I and II, and CD1, co-stimulatory markers like CD40, CD80 (B7-1), and CD86 (B7-2), ICAM-1, and produce various cytokines like MMP-2, -3, -9, IL-1 $\beta$ , -6, -18, etc.<sup>165</sup>

In recent decades, ultra-pH-responsive microneedle arrays have been used for cancer immunotherapy in animal models.<sup>166</sup> Thuy and co-workers developed a nano-engineered DNA vaccine and loaded it on polyethylene glycol/ aminoester urethane in tumorized mice with B16/OVA melanoma cells. They showed that viral DNA was successfully released into the subcutaneous region due to its ultra-pH-responsive nature. After insertion of exogenous sequence and synthesis of target protein, the activation of Toll-like receptor signaling pathway and MAPK/JNK and JAK/STAT axes induced MHC class I production thus a large number of CD8<sup>+</sup> lymphocytes was recruited and promoted antibody-dependent cancer immunity (Figure 8).<sup>165,166</sup> To elicit immunization via using inactivated antigens and MN technology, Choi et al.<sup>167</sup> fabricated a separable/coated MNs delivering canine influenza vaccine to the hairy skin in a

canine model. The tips of MNs were made by hyaluronic acid/sucrose/Tween80 followed by dip-coated in vaccine solution. The vaccine solution is composed of polyvinyl alcohol and inactivated VC378 vaccine.<sup>167</sup> In this system, the base of MNs was fabricated using PCL, allowing long-term attachment of MNs. Of note, the dissolvable tips were separated following insertion within less than 10 s. About 100% coated vaccine was efficiently delivered on hairy skin.<sup>167</sup> This MN delivery system caused antibody production similar to conventional intramuscular injection 28 days after twice the treatments.<sup>167</sup> Due to improving vaccine coated MN delivery system, Choi et al.<sup>168</sup> developed a PLA-based MN coated using PVA/trehalose for delivery of smallpox virus and reduced inactivated virus for suitable immunogenicity. Data showed that vacuum-dried coated MNs have higher stability and wettability, enhancing the distribution of vaccines into the deep layers.<sup>168</sup> Furthermore, the PVA/trehalose/smallpox-coated MN showed increased stability within 6 months at  $-20^{\circ}\text{C}$  and 1 month at  $4^{\circ}\text{C}$ .<sup>154</sup> According to *in vivo* experiments, the designed coated MNs promoted both humoral and cell-mediated immune responses while increasing IFN- $\gamma$  content.<sup>168</sup>

Compared to protein-based vaccines, nucleic acid-based vaccines have limitations like high-cost protein purification methods, inappropriate protein folding, and limited antigen delivery.<sup>169</sup> However, the permanent exotic DNA integration may be cause self-antigen production and auto-immune diseases. Non-viral vectors like cationic polymer, inorganic nanoparticles, and liposomes are interesting carriers due to proper immune stimulation, easy production, and providing larger loading capacity; however, degradation via serum endonuclease and stability for a more extended period is still challenging.<sup>169</sup> To examine the influence of nano-carriers and MN delivery systems on the efficient DNA vaccine delivery, Duong and co-workers developed an MN array coated by pH-sensitive multilayer polyelectrolytes enriched with heparin, OSM-b-PEG-b-PAEU copolymers, polyplex, and DNA vaccines for Alzheimer's therapy applicants. The pH at the range of physiological conditions contributes to the disassembly between negatively charged heparin and copolymers, promoting polyplex liberation. It was shown that this system delivered the total content of polyplex within 5 min in *in vitro* conditions. The detachment of polyplex was also indicated in MNs after insertion into the cutaneous tissue. According to data, the target DNA can be efficiently delivered to the mouse dermal layer when MNs with  $330\ \mu\text{m}$ -length needles were used. Following DNA release and synthesis of A $\beta$  peptides, anti-A $\beta$  IgG titer was increased as compared to conventional injection.<sup>170</sup>

In protein-based vaccines, recombinant protein subunits of the target pathogen have been produced *in vitro*.<sup>155</sup> Compared to nucleic acid-based vaccines, protein-based vaccines have illustrated fewer safety issues because of nucleic acid absence and non-integration to the cellular

genome permanently.<sup>155</sup> Generally, the recombinant proteins have been delivered along with adjuvants to induce an immune response.<sup>152</sup> In this regard, Kuwentrai et al.<sup>171</sup> designed dissolvable hyaluronic acid-based MNs with an aluminum hydroxide gel adjuvant to deliver the S1-RBD domain of coronavirus spike protein. Based on data, the MN delivery system facilitated S1-RBD domain delivery as fast as 10 s in  $330\ \mu\text{m}$  depth of the skin.<sup>171</sup> The transfer of the S1-RBD domain led to the activation of humoral mediated and cell-mediated response significantly *in vivo* within 3 months after three-time vaccination.<sup>171</sup> Probable severe inflammation may occur due to enhanced antibody production in some cases making peptide-based vaccines include B or T lymphocytes epitopes to induce a mild immune reaction.<sup>152</sup> In an experiment conducted by Chen et al.,<sup>172</sup> they loaded F1 protein of *Yersinia pestis* in the polyethylene glycol (PEG)-modified lipoparticles delivering via commercial plastic-based MNs for vaccination against plague. According to data, the IgG antibody titer was increased highly within 45 days in the plasma of treated mice without significant effects on body weight.<sup>172</sup> Moreover, INF- $\gamma$ , TNF $\alpha$ , and IL-4 were also enhanced insignificantly in mice that received MN plus liposome-loaded F1 protein.<sup>172</sup> The MN delivery system via liposome-loaded F1 protein subunit exhibited an effective humoral and cell-mediated immunity with prominent safety.<sup>172</sup>

## Microneedle technologies in the context of regenerative medicine

Application of complex and sophisticated fabrication tools with a wide range of materials in the development of MN patches can support local, controllable drug release, several therapeutic factors, and certain cells across cutaneous tissue to the target sites in a broad spectrum of conditions.<sup>173</sup> In a recent experiment, it was shown that ovalbumin-induced dendritic cells loaded inside cryogenic needles can promote antigen processing, leading to tumor mass atresia and the prevention of metastatic cells into the circulation system.<sup>173</sup> Along with these statements, MN patches are suitable candidates for the restoration of injured tissue. The efficiency and regenerative potential of MN patches have been proved in terms of wound healing, neovascularization, and artificial organ reconstruction.<sup>174,175</sup> For instance, epicedial attachment of fibrin-coated MN patches harboring cardiac stromal cells promoted cardiac regeneration in a rat model of myocardial infarction.<sup>176</sup> It was suggested that this system can induce cardiac regeneration via the development of micro-sized channels that transfer the secretome of cardiac stromal cells into the ischemic sites. Histological analysis revealed the promotion of vascularization along with cardiogenesis at the infarcted site, leading to a reduction of scar size.<sup>176</sup> Considering the potency of the MN patch system and its efficiency in different conditions, some researchers used this delivery system in the

**Table 2.** Some list of MN patch clinical trials recorded up to January 2022 (available at <https://clinicaltrials.gov/us>).

Status	Object	Phase
Enrolling by invitation	Brightening cutaneous tissue using MN in individuals with solar Lentiginos	Not Applicable
Completed	Local delivery of Lidocaine for oral anesthesia using MN	Phase I
Completed	Vaccination against viruses in healthy infants/young children using MN	Not Applicable
Completed	Diabetes diagnosis and glucose monitoring using MN	Not Applicable
Unknown	MN for the treatment of psoriatic plaques	Not Applicable
Suspended	Pilocarpine microneedles for sweat induction in cystic fibrosis patients using MN	Not Applicable
Completed	Vaccination against influenza	Phase I
Recruiting	Vaccination against measles and rubella	Phases I and II
Recruiting	Efficacy of transdermal microneedle patch for topical anesthesia enhancement in pediatric thalassemia patients	Phase II
Recruiting	MN for delivery of Doxorubicin in patients with cutaneous T-cell Lymphoma	Phase I
Completed	Dose-limiting toxicity and maximum tolerated dose of MN containing Doxorubicin in basal cell carcinoma	Phase I
Recruiting	Evaluation of cutaneous micropores after application of MN	Not Applicable
Completed	Physiological study to determine the allergic skin activity after different skin preparation using MN	Phase I
Completed	Pain and safety of microneedles in oral cavity	Not Applicable
Completed	Minimally invasive sensing of beta-lactam antibiotics	Phase I
Unknown	Microneedle and trichloroacetic acid in treatment of melasma	Not Applicable
Recruiting	Microneedles for diagnosis of latent tuberculosis	Not Applicable
Unknown	Microneedle radiofrequency for moderate-to-severe acne vulgaris	Not Applicable

MN: microneedle patch.

restoration of injured bone tissue in both in vivo and in vitro settings. The micro-anatomical regulation of injured tissue regeneration using a combination of scaffold with specific cell lineages such as mesenchymal stem cells can lead to aligned cell polarization in the affected sites. Besides, the tight manner release of certain growth factors such as vascular endothelial growth factor, stromal-derived factor 1 $\alpha$ , and bone morphogenetic protein-2 can increase osteogenic and angiogenic capacity of transplanted cells.<sup>177</sup> These data show that MN alone or in combination with conventional engineering systems can increase regenerative potential. Transdermal application of detachable MN patches with encapsulated mesenchymal stem cells inside gelatin methacryloyl promoted epithelialization and inhibited scar size propagation via accelerating vascularization compared to direct transdermal injection.<sup>178</sup> Taken together, it is noteworthy to mention that MN patch have opened new approach in regenerative medicine based on providing biomimetic cell niche by the regulation of signaling molecules agents to the targeted sites region. It seems that studies in this area are in infancy and incomplete. For application and establishment of MN patch based cell therapies numerous future studies are mandatory.

### Clinical application of MNs

Over the recent years, numerous preclinical studies and clinical trials have been executed to investigate the safety, stability, and functionality of designed MN patches and commercially fabricated MN arrays for intradermal delivery

approaches (Table 2).<sup>55,179,180</sup> Based on clinical trials listed at [www.clinicaltrials.gov/us](http://www.clinicaltrials.gov/us), the designed MNs were examined for skin disorders, local anesthesia, vaccine delivery, glucose monitoring, and biosensing purposes.<sup>179,180</sup> In a clinical trial study, the systemic contents of glucose were continuously monitored in healthy volunteers and type 1 diabetic patients using solid MN array-based sensors based on interstitial glucose levels.<sup>181</sup> Based on data outlined in Table 2, the residual of certain compounds such as beta-lactam antibiotics was also detected as a minimally invasive approach.<sup>182</sup> It was suggested that the application of MN patches on the surface of cutaneous tissue is an invasive and simple approach for the collection of samples compared to pulling out interstitial fluids. In a recently conducted clinical trial study, the quality of samples obtained via MN patches, in terms of RNA sequencing, as compared to the conventional biopsy approach from the skin. Nevertheless, the results have not been documented yet.<sup>183</sup> Data support the eligibility of MN patches for vaccination of individuals against various infectious agents such as influenza, measles, rubella, etc. In line with these statements, insulin has been successfully delivered via hollow MNs in diabetic patients.<sup>180</sup> Considering recent data, it is noteworthy to mention that MN patches with different geometrical values and designs are a suitable delivery approach for the treatment of different pathological conditions. Additionally, by combining different scientific disciplines MN patches can be developed in a way to use for biosensing, sampling, releasing, and monitoring purposes with a minimal invasion to the cutaneous tissue. Of note, the application of MN patches for

topical delivery seems very suitable and can avoid side effects associated with systemic delivery of certain therapeutic agents.

## Challenges and perspectives of MNs

Despite the potency of different MN types in the delivery of target molecules into an intradermal layer or hypodermic region,<sup>184,185</sup> some issues limit the extensive application of MN-based delivery in the clinical setting. In the present time, the fabrication systems used for MN device preparation need a new design to diminish economic costs.<sup>186</sup> The efficiency of MNs in drug delivery and vaccination has not been fully addressed and further studies should be conducted accordingly. Regarding complicated and several fabrication steps, sterilization, and disinfection of MNs are new challenges.<sup>187</sup> These procedures should be in a way not affect the therapeutic efficiency of cargo and factors. Pre-treatment of MNs with most heat, irradiations, or other factors can neutralize MN delivery capacity and/or therapeutic outcome in *in vivo* niches.<sup>188</sup> In most studies, the repeatability and efficacy of MN devices have not been fully assessed and cGMP and quality control should be precisely defined.<sup>186</sup> Considering the existence of person-to-person differences in the terms of cutaneous layer thickness, MNs with similar geometrical values may yield varied therapeutic outcomes. Other factors with potency to affect delivery capacity are needle tip diameter and sharpness.<sup>189</sup> Notably, the application of suitable force in a controlled manner seems to be vital for the dynamic activity of cargo in the desired period. Excessive tip sharpness can lead to needle instability. In line with these statements, the penetration depth of needles has not been carefully analyzed. Based on the dynamic acidity of cargo, the depth insertion can be altered. The density of needle per cm<sup>2</sup> of MN surface is also identical in the timely delivery of cargo into the target sites.<sup>190</sup> Again, this parameter is affected by materials used for MN patch synthesis and the shelf life of cargo. The loading capacity of needles is so variable according to the different MN fabrication systems. This issue can make it difficult to calculate the loading level per needle (dosage) and delivery efficiency. Whether short- and long-term contact of MN patches inside cutaneous tissue can lead to unwanted side effects has not been evaluated in a large-scale population. For example, biodegradable porous silicon MNs can be easily broken after insertion into the hypoderm.<sup>191</sup> Commensurate with these descriptions, obtaining the comprehensive concept of drug therapy using MN patches faces numerous technical limitations in terms of fabrication, and drug delivery efficiency.

## Conclusions

The application of MN devices has opened hopes in the sustained release of therapeutic agents via cutaneous

tissue. Several aspects of MN-based delivery have been uncovered that paved the way for novel therapeutic modalities. Further attempts supporting the understanding of mechanisms associated with efficient delivery are highly needed. Considering the existence of inherent limitations in the area of transdermal MN-based delivery, further investigations should address these issues as possible.

## Author contributions

F.N.A., S.S., L.S., H.A., S.F.K., K.M., and E.S. prepared draft and collected data. R.R. supervised the study.

## Declaration of conflicting interests

The author(s) declared no potential conflicts of interest with respect to the research, authorship, and/or publication of this article.

## Funding

The author(s) received no financial support for the research, authorship, and/or publication of this article.

## ORCID iDs

Sepideh Saghati  <https://orcid.org/0000-0002-2801-3482>

Sonia Fathi Karkan  <https://orcid.org/0000-0002-1712-9367>

Reza Rahbarghazi  <https://orcid.org/0000-0003-3864-9166>

## References

1. Waghule T, Singhvi G, Dubey SK, et al. Microneedles: A smart approach and increasing potential for transdermal drug delivery system. *Biomed Pharmacother* 2019; 109: 1249–1258.
2. Zhu J, Zhou X, Libanori A, et al. Microneedle-based bioassays. *Nano Adv* 2020; 2: 4295–4304.
3. Queiroz MLB, Shanmugam S, Santos LNS, et al. Microneedles as an alternative technology for transdermal drug delivery systems: a patent review. *Expert Opin Ther Pat* 2020; 30: 433–452.
4. Shwayder T and Akland T. Neonatal skin barrier: structure, function, and disorders. *Dermatol Ther* 2005; 18: 87–103.
5. Hao Y, Li W, Zhou X, et al. Microneedles-based transdermal drug delivery systems: a review. *J Biomed Nanotechnol* 2017; 13: 1581–1597.
6. Escobar-Chávez JJ, Bonilla-Martínez D, Angélica M, et al. Microneedles: a valuable physical enhancer to increase transdermal drug delivery. *J Clin Pharmacol* 2011; 51: 964–977.
7. Brown MB, Martin GP, Jones SA, et al. Dermal and transdermal drug delivery systems: current and future prospects. *Drug Deliv* 2006; 13: 175–187.
8. Mitragotri S, Burke PA and Langer R. Overcoming the challenges in administering biopharmaceuticals: formulation and delivery strategies. *Nat Rev Drug Discov* 2014; 13: 655–672.
9. Larrañeta E, McCrudden MT, Courtenay AJ, et al. Microneedles: a new frontier in nanomedicine delivery. *Pharm Res* 2016; 33: 1055–1073.

10. Mittapally S, Taranum R and Parveen S. Microneedles-a potential transdermal drug delivery. *Int J Pharma Res Health Sci* 2018; 6: 2579–2585.
11. Lee JW, Choi SO, Felner EI, et al. Dissolving microneedle patch for transdermal delivery of human growth hormone. *Small* 2011; 7: 531–539.
12. Larrañeta E, Lutton REM, Woolfson AD, et al. Microneedle arrays as transdermal and intradermal drug delivery systems: materials science, manufacture and commercial development. *Mater Sci Eng R Rep* 2016; 104: 1–32.
13. Dabbagh SR, Sarabi MR, Rahbarghazi R, et al. 3D-printed microneedles in biomedical applications. *iScience* 2021; 24: 102012.
14. Puri A, Nguyen HX, Tijani AO, et al. Characterization of microneedles and microchannels for enhanced transdermal drug delivery. *Ther Deliv* 2021; 12: 77–103.
15. Long L-Y, Zhang J, Yang Z, et al. Transdermal delivery of peptide and protein drugs: strategies, advantages and disadvantages. *J Drug Deliv Sci Tech* 2020; 60: 102007.
16. Rodríguez-Cruz IM, Domínguez-Delgado CL, Escobar-Chávez JJ, et al. Physical penetration enhancers: an overview. In: Escobar-Chávez JJ (ed.) *Current Technologies to Increase the Transdermal Delivery*. Dubai: Bentham Science Publishers, 2016, pp.3–34.
17. Roustit M, Blaise S and Cracowski JL. Trials and tribulations of skin iontophoresis in therapeutics. *Br J Clin Pharmacol* 2014; 77: 63–71.
18. Dixit N, Bali V, Baboota S, et al. Iontophoresis – an approach for controlled drug delivery: a review. *Curr Drug Deliv* 2007; 4: 1–10.
19. Wang Y, Zeng L, Song W, et al. Influencing factors and drug application of iontophoresis in transdermal drug delivery: an overview of recent progress. *Drug Deliv Transl Res* 2022; 12: 15–26.
20. Seah BC and Teo BM. Recent advances in ultrasound-based transdermal drug delivery. *Int J Nanomedicine* 2018; 13: 7749–7763.
21. Sennoga CA, Kanbar E, Auboire L, et al. Microbubble-mediated ultrasound drug-delivery and therapeutic monitoring. *Expert Opin Drug Deliv* 2017; 14: 1031–1043.
22. Medi BM, Layek B and Singh J. Electroporation for dermal and Transdermal Drug Delivery. In: N Dragicevic, HI Maibach (eds) *Percutaneous penetration enhancers physical methods in penetration enhancement*. Berlin, Heidelberg: Springer Berlin Heidelberg, 2017, pp.105–122.
23. Sokolowska E and Błachnio-Zabielska AU. A critical review of electroporation as a plasmid delivery system in mouse skeletal muscle. *Int J Mol Sci* 2019; 20: 2776.
24. Waibel JS, Rudnick A, Shagalov DR, et al. Update of ablative fractionated lasers to enhance cutaneous topical drug delivery. *Adv Ther* 2017; 34: 1840–1849.
25. Haak CS, Hannibal J, Paasch U, et al. Laser-induced thermal coagulation enhances skin uptake of topically applied compounds. *Lasers Surg Med* 2017; 49: 582–591.
26. Li Y, Guo L and Lu W. Laser ablation-enhanced transdermal drug delivery. *Photonics Lasers Med* 2013; 2: 315–322.
27. Serrano-Castañeda P, Escobar-Chavez JJ, Rodriguez-cruz IM, et al. Microneedles as enhancer of drug absorption through the skin and applications in medicine and cosmetology. *J Pharm Pharm Sci* 2018; 21: 73–93.
28. Haq MI, Smith E, John DN, et al. Clinical administration of microneedles: skin puncture, pain and sensation. *Biomed Microdevices* 2009; 11: 35–47.
29. Gill HS and Prausnitz MR. Pocketed microneedles for drug delivery to the skin. *J Phys Chem Solids* 2008; 69: 1537–1541.
30. Williams AC and Barry BW. Penetration enhancers. *Adv Drug Deliv Rev* 2012; 64: 128–137.
31. Zheng P, Chen L, Yuan X, et al. Exosomal transfer of tumor-associated macrophage-derived miR-21 confers cisplatin resistance in gastric cancer cells. *J Exp Clin Cancer Res* 2017; 36: 53.
32. Panda A, Matadh VA, Suresh S, et al. Non-dermal applications of microneedle drug delivery systems. *Drug Deliv Transl Res* 2022; 12: 67–78.
33. Tang B and Sato K. Advanced surfactant-modified wet anisotropic etching. In: Islam N (ed.) *Microelectromechanical systems and devices*. IntechOpen, 2012, p.131.
34. Cheng H, Liu M, Du X, et al. Recent progress of microneedle formulations: fabrication strategies and delivery applications. *J Drug Deliv Sci Tech* 2019; 50: 18–26.
35. Xie L, Zeng H, Sun J, et al. Engineering microneedles for therapy and diagnosis: a survey. *Micromachines* 2020; 11: 271.
36. Vogelaar L, Barsema JN, van Rijn CJ, et al. Phase separation micromolding—PS $\mu$ M. *Adv Mater Weinheim* 2003; 15: 1385–1389.
37. Verma A, Jennings J, Johnson RD, et al. Fabrication of 3D charged particle trap using through-silicon vias etched by deep reactive ion etching. *J Vac Sci Technol B Nanotechnol Microelectron Mater Process Meas Phenom* 2013; 31: 032001.
38. Jansen H, Gardeniers H, Boer MD, et al. A survey on the reactive ion etching of silicon in microtechnology. *J Micromech Microeng* 1996; 6: 14–28.
39. Gentili E, Tagaglio L and Aggogeri F. Review on micromachining techniques. In: Kuljanic E (ed.) *AMST'05 advanced manufacturing systems and technology*. New York: Springer, 2005, pp.387–396.
40. Zhu D and Zeng YB. Micro electroforming of high-aspect-ratio metallic microstructures by using a movable mask. *CIRP Annals* 2008; 57: 227–230.
41. Chen Y-T, Liao Y-S and Chen T-T. Fabrication of arrayed microneedles by laser LIGA process (Laser processing). In: *Proceedings of international conference on leading edge manufacturing in 21st century: LEM21 20051*, 2005, pp.285–290. Nagoya: The Japan Society of Mechanical Engineers.
42. Leone M, Mönkäre J, Bouwstra JA, et al. Dissolving microneedle patches for dermal vaccination. *Pharm Res* 2017; 34: 2223–2240.
43. Rizvi NH and Apte P. Developments in laser micro-machining techniques. *J Mater Process Technol* 2002; 127: 206–210.
44. Aoyagi S, Izumi H, Isono Y, et al. Laser fabrication of high aspect ratio thin holes on biodegradable polymer and its application to a microneedle. *Sens Actuators A Phys* 2007; 139: 293–302.
45. Economidou SN, Uddin MJ, Marques MJ, et al. A novel 3D printed hollow microneedle microelectromechanical sys-

- tem for controlled, personalized transdermal drug delivery. *Addit Manuf* 2021; 38: 101815.
46. Hu Z, Meduri CS, Ingrole RSJ, et al. Solid and hollow metallic glass microneedles for transdermal drug-delivery. *Appl Phys Lett* 2020; 116: 203703.
47. Butz KD, Griebel AJ, Novak T, et al. Prestress as an optimal biomechanical parameter for needle penetration. *J Biomech* 2012; 45: 1176–1179.
48. Sivamani RK, Stoeber B, Liepmann D, et al. Microneedle penetration and injection past the stratum corneum in humans. *J Dermatol Treat* 2009; 20: 156–159.
49. Kalluri H, Choi S-O, Guo XD, et al. Evaluation of microneedles in human subjects. In: Dragicevic N and Maibach HI (eds) *Percutaneous penetration enhancers physical methods in penetration enhancement*. Springer, 2017, pp.325–340.
50. Olatunji O, Das DB, Garland MJ, et al. Influence of array interspacing on the force required for successful microneedle skin penetration: theoretical and practical approaches. *J Pharm Sci* 2013; 102: 1209–1221.
51. Kang N-W, Kim S, Lee J-Y, et al. Microneedles for drug delivery: recent advances in materials and geometry for pre-clinical and clinical studies. *Expert Opin Drug Deliv* 2021; 18: 929–947.
52. Petchsangsa M, Rojanarata T, Opanasopit P, et al. The combination of microneedles with electroporation and sonophoresis to enhance hydrophilic macromolecule skin penetration. *Biol Pharm Bull* 2014; 37: 1373–1382.
53. Ingrole RSJ and Gill HS. Microneedle coating methods: a review with a perspective. *J Pharmacol Exp Ther* 2019; 370: 555–569.
54. Kapoor Y, Milewski M, Dick L, et al. Coated microneedles for transdermal delivery of a potent pharmaceutical peptide. *Biomed Microdevices* 2019; 22: 7–10.
55. Nguyen TT, Oh Y, Kim Y, et al. Progress in microneedle array patch (MAP) for vaccine delivery. *Hum Vaccin Immunother* 2020; 17: 316–327.
56. Castilla-Casadiago DA, Carlton H, Gonzalez-Nino D, et al. Design, characterization, and modeling of a chitosan microneedle patch for transdermal delivery of meloxicam as a pain management strategy for use in cattle. *Mater Sci Eng C* 2021; 118: 111544.
57. Smith HS and Baird W. Meloxicam and selective COX-2 inhibitors in the management of pain in the palliative care population. *Am J Hosp Palliat Med* 2003; 20: 297–306.
58. Ramalheiro A, Paris JL, Silva BFB, et al. Rapidly dissolving microneedles for the delivery of cubosome-like liquid crystalline nanoparticles with sustained release of rapamycin. *Int J Pharm* 2020; 591: 119942.
59. Gao M and Si X. Rapamycin ameliorates psoriasis by regulating the expression and methylation levels of tropomyosin via ERK1/2 and mTOR pathways in vitro and in vivo. *Exp Dermatol* 2018; 27: 1112–1119.
60. Ogawa E, Sato Y, Minagawa A, et al. Pathogenesis of psoriasis and development of treatment. *J Dermatol* 2018; 45: 264–272.
61. Buerger C. Epidermal mTORC1 signaling contributes to the pathogenesis of psoriasis and could serve as a therapeutic target. *Front Immunol* 2018; 9: 2786.
62. Pukfukdee P, Banlunara W, Rutwaree T, et al. Solid composite material for delivering viable cells into skin tissues via detachable dissolvable microneedles. *ACS Appl Bio Mater* 2020; 3: 4581–4589.
63. Eum J, Kim Y, Um DJ, et al. Solvent-free polycaprolactone dissolving microneedles generated via the thermal melting method for the sustained release of capsaicin. *Micromachines* 2021; 12: 167.
64. Zhang Y, Deng X, Lei T, et al. Capsaicin inhibits proliferation and induces apoptosis in osteosarcoma cell lines via the mitogen-activated protein kinase pathway. *Oncol Rep* 2017; 38: 2685–2696.
65. Li W, Terry RN, Tang J, et al. Rapidly separable microneedle patch for the sustained release of a contraceptive. *Nat Biomed Eng* 2019; 3: 220–229.
66. Nagarkar R, Singh M, Nguyen HX, et al. A review of recent advances in microneedle technology for transdermal drug delivery. *J Drug Deliv Sci Tech* 2020; 59: 101923.
67. Pamornpathomkul B, Niyomtham N, Yingyongnarongkul B-E, et al. Cationic niosomes for enhanced skin immunization of plasmid DNA-encoding ovalbumin via hollow microneedles. *AAPS PharmSciTech* 2018; 19: 481–488.
68. Uppuluri C, Shaik AS, Han T, et al. Effect of microneedle type on transdermal permeation of rizatriptan. *AAPS PharmSciTech* 2017; 18: 1495–1506.
69. Cárcamo-Martínez Á, Mallon B, Anjani QK, et al. Enhancing intradermal delivery of tofacitinib citrate: comparison between powder-loaded hollow microneedle arrays and dissolving microneedle arrays. *Int J Pharm* 2021; 593: 120152.
70. McAlister E, Dutton B, Vora LK, et al. Directly compressed tablets: A novel drug-containing reservoir combined with hydrogel-forming microneedle arrays for transdermal drug delivery. *Adv Healthc Mater* 2021; 10: e2001256.
71. Chew SW, Shah AH, Zheng M, et al. A self-adhesive microneedle patch with drug loading capability through swelling effect. *Bioeng Transl Med* 2020; 5: e10157.
72. Yang G, He M, Zhang S, et al. An acryl resin-based swellable microneedles for controlled release intradermal delivery of granisetron. *Drug Dev Ind Pharm* 2018; 44: 808–816.
73. Marx W, Ried K, McCarthy AL, et al. Ginger-mechanism of action in chemotherapy-induced nausea and vomiting: a review. *Crit Rev Food Sci Nutr* 2017; 57: 141–146.
74. Dreiss CA. Hydrogel design strategies for drug delivery. *Curr Opin Colloid Interface Sci* 2020; 48: 1–17.
75. Zhang Y, Yu J, Bomba HN, et al. Mechanical force-triggered drug delivery. *Chem Rev* 2016; 116: 12536–12563.
76. Raza A, Rasheed T, Nabeel F, et al. Endogenous and exogenous stimuli-responsive drug delivery systems for programmed site-specific release. *Molecules* 2019; 24: 1117.
77. Schmaljohann D. Thermo- and pH-responsive polymers in drug delivery. *Adv Drug Deliv Rev* 2006; 58: 1655–1670.
78. Li Z and Guan J. Thermosensitive hydrogels for drug delivery. *Expert Opin Drug Deliv* 2011; 8: 991–1007.
79. Tobin KV, Fiegel J and Brogden NK. Thermosensitive gels used to improve microneedle-assisted transdermal delivery of naltrexone. *Polymers* 2021; 13: 933.
80. Zhu YJ and Chen F. PH-responsive drug-delivery systems. *Chem Asian J* 2015; 10: 284–305.
81. Xie J, Li A and Li J. Advances in pH-sensitive polymers for smart insulin delivery. *Macromol Rapid Commun* 2017; 38: 1700413.

82. Ke CJ, Lin Y-J, Hu YC, et al. Multidrug release based on microneedle arrays filled with pH-responsive PLGA hollow microspheres. *Biomaterials* 2012; 33: 5156–5165.
83. Huang Z, Lin S, Long C, et al. Notch signaling pathway mediates doxorubicin-driven apoptosis in cancers. *Cancer Manag Res* 2018; 10: 1439–1448.
84. Miao D, Yu Y, Chen Y, et al. Facile construction of i-Motif DNA-conjugated gold nanostars as near-infrared and pH dual-responsive targeted drug delivery systems for combined cancer therapy. *Mol Pharm* 2020; 17: 1127–1138.
85. Qian H, Zhang Y, Wu B, et al. Structure and function of HECT E3 ubiquitin ligases and their role in oxidative stress. *J Transl Int Med* 2020; 8: 71–79.
86. Zhang X, Chen G, Liu Y, et al. Black phosphorus-loaded separable microneedles as responsive oxygen delivery carriers for wound healing. *ACS Nano* 2020; 14: 5901–5908.
87. Baltzis D, Eleftheriadou I and Veves A. Pathogenesis and treatment of impaired wound healing in diabetes mellitus: new insights. *Adv Ther* 2014; 31: 817–836.
88. Cano Sanchez M, Lancel S, Boulanger E, et al. Targeting oxidative stress and mitochondrial dysfunction in the treatment of impaired wound healing: a systematic review. *Antioxidants* 2018; 7: 98.
89. Tham HP, Xu K, Lim WQ, et al. Microneedle-assisted topical delivery of photodynamically active mesoporous formulation for combination therapy of deep-seated melanoma. *ACS Nano* 2018; 12: 11936–11948.
90. Zhao X, Li X, Zhang P, et al. Tip-loaded fast-dissolving microneedle patches for photodynamic therapy of subcutaneous tumor. *J Control Release* 2018; 286: 201–209.
91. Linsley CS and Wu BM. Recent advances in light-responsive on-demand drug-delivery systems. *Ther Deliv* 2017; 8: 89–107.
92. Fang J-H, Liu C-H, Hsu R-S, et al. Transdermal composite microneedle composed of mesoporous iron oxide nanoparticle and PVA for androgenetic alopecia treatment. *Polymers* 2020; 12: 1392.
93. Katzer T, Leite Junior A, Beck R, et al. Physiopathology and current treatments of androgenetic alopecia: going beyond androgens and anti-androgens. *Dermatol Ther* 2019; 32: e13059.
94. Messenger AG and Rundegren J. Minoxidil: mechanisms of action on hair growth. *Br J Dermatol* 2004; 150: 186–194.
95. Zandi A, Khayamian MA, Saghafi M, et al. Microneedle-based generation of microbubbles in cancer tumors to improve ultrasound-assisted drug delivery. *Adv Healthc Mater* 2019; 8: e1900613.
96. Ren X, Zhao B, Chang H, et al. Paclitaxel suppresses proliferation and induces apoptosis through regulation of ROS and the AKT/MAPK signaling pathway in canine mammary gland tumor cells. *Mol Med Rep* 2018; 17: 8289–8299.
97. Banga AK, Bose S and Ghosh TK. Iontophoresis and electroporation: comparisons and contrasts. *Int J Pharm* 1999; 179: 1–19.
98. Henley JL. Iontophoretic drug delivery electrodes and method. Google patents, US6895271B2, 2000.
99. Wang Y and Kohane DS. External triggering and triggered targeting strategies for drug delivery. *Nat Rev Mater* 2017; 2: 1–14.
100. Yang J, Li Y, Ye R, et al. Smartphone-powered iontophoresis-microneedle array patch for controlled transdermal delivery. *Microsyst Nanoeng* 2020; 6: 112.
101. Fuchs S, Shariati K and Ma M. Stimuli-responsive insulin delivery devices. *Pharm Res* 2020; 37: 202.
102. Zhang Y, Yu J, Wang J, et al. Thrombin-responsive transcutaneous patch for auto-anticoagulant regulation. *Adv Mater Weinheim* 2017; 29: 1604043.
103. Tao W and He Z. ROS-responsive drug delivery systems for biomedical applications. *Asian J Pharm Sci* 2018; 13: 101–112.
104. Tong Z, Zhou J, Zhong J, et al. Glucose- and H<sub>2</sub>O<sub>2</sub>-responsive polymeric vesicles integrated with microneedle patches for glucose-sensitive transcutaneous delivery of insulin in diabetic rats. *ACS Appl Mater Interfaces* 2018; 10: 20014–20024.
105. LaVan DA, McGuire T and Langer R. Small-scale systems for in vivo drug delivery. *Nat Biotechnol* 2003; 21: 1184–1191.
106. He Y, Hong C, Li J, et al. Synthetic charge-invertible polymer for rapid and complete implantation of layer-by-layer microneedle drug films for enhanced transdermal vaccination. *ACS Nano* 2018; 12: 10272–10280.
107. Haj-Ahmad R, Khan H, Arshad MS, et al. Microneedle coating techniques for transdermal drug delivery. *Pharmaceutics* 2015; 7: 486–502.
108. Chen M-C, Ling M-H, Lai K-Y, et al. Chitosan microneedle patches for sustained transdermal delivery of macromolecules. *Biomacromolecules* 2012; 13: 4022–4031.
109. Kim Y-C, Quan F-S, Compans RW, et al. Stability kinetics of influenza vaccine coated onto microneedles during drying and storage. *Pharm Res* 2011; 28: 135–144.
110. Lau S, Fei J, Liu H, et al. Multilayered pyramidal dissolving microneedle patches with flexible pedestals for improving effective drug delivery. *J Control Release* 2017; 265: 113–119.
111. Ameri M, Daddona PE and Maa Y-F. Demonstrated solid-state stability of parathyroid hormone PTH(1–34) coated on a novel transdermal microprojection delivery system. *Pharm Res* 2009; 26: 2454–2463.
112. Daddona PE, Matriano JA, Mandema J, et al. Parathyroid hormone (1–34)-coated microneedle patch system: clinical pharmacokinetics and pharmacodynamics for treatment of osteoporosis. *Pharm Res* 2011; 28: 159–165.
113. Ye Y, Yu J, Wang C, et al. Microneedles integrated with pancreatic cells and synthetic glucose-signal amplifiers for smart insulin delivery. *Adv Mater Weinheim* 2016; 28: 3115–3121.
114. Choi S-O, Kim YC, Park J-H, et al. An electrically active microneedle array for electroporation. *Biomed Microdevices* 2010; 12: 263–273.
115. Khullar M, Cheema BS and Raut SK. Emerging evidence of epigenetic modifications in vascular complication of diabetes. *Front Endocrinol* 2017; 8: 237.
116. Pouwer F. Depression: a common and burdensome complication of diabetes that warrants the continued attention of clinicians, researchers and healthcare policy makers. *Diabetologia* 2017; 60: 30–34.
117. Simó-Servat O, Hernández C and Simó R. Diabetic retinopathy in the context of patients with diabetes. *Ophthalmic Res* 2019; 62: 211–217.

118. Zimmet P, Alberti KG, Magliano DJ, et al. Diabetes mellitus statistics on prevalence and mortality: facts and fallacies. *Nat Rev Endocrinol* 2016; 12: 616–622.
119. GhavamiNejad A, Lu B, Samarikhajaj M, et al. Transdermal delivery of a somatostatin receptor type 2 antagonist using microneedle patch technology for hypoglycemia prevention. *Drug Deliv Transl Res* 2021; 2021: 1–13.
120. Zhu S, Zhang B, Wang Y, et al. A bilayer microneedle for therapeutic peptide delivery towards the treatment of diabetes in db/db mice. *J Drug Deliv Sci Tech* 2021; 62: 102336.
121. Roy L and Bhattacharjee M. Overview of novel routes of insulin: current status. *Int J Adv Med* 2020; 7: 1597.
122. Yadav PR and Pattanayek SK. Modulation of physicochemical properties of polymers for effective insulin delivery systems. In: Chandra P and Pandey LM (eds) *Biointerface engineering: prospects in medical diagnostics and drug delivery*. Springer, 2020, pp.123–148.
123. Kim S, Yang H, Eum J, et al. Implantable powder-carrying microneedles for transdermal delivery of high-dose insulin with enhanced activity. *Biomaterials* 2020; 232: 119733.
124. Chen BZ, Zhang LQ, Xia YY, et al. A basal-bolus insulin regimen integrated microneedle patch for intraday postprandial glucose control. *Sci Adv* 2020; 6: eaba7260.
125. Chen G, Yu J and Gu Z. Glucose-responsive microneedle patches for diabetes treatment. *J Diabetes Sci Technol* 2019; 13: 41–48.
126. Yu J, Zhang Y, Yan J, et al. Advances in bioresponsive closed-loop drug delivery systems. *Int J Pharm* 2018; 544: 350–357.
127. Chen S, Miyazaki T, Itoh M, et al. Temperature-stable boronate gel-based microneedle technology for self-regulated insulin delivery. *ACS Appl Polym Mater* 2020; 2: 2781–2790.
128. Yu J, Zhang Y, Ye Y, et al. Microneedle-array patches loaded with hypoxia-sensitive vesicles provide fast glucose-responsive insulin delivery. *Proc Natl Acad Sci* 2015; 112: 8260–8265.
129. Ullah A, Choi HJ, Jang M, et al. Smart microneedles with porous polymer layer for glucose-responsive insulin delivery. *Pharmaceutics* 2020; 12: 606.
130. Singh RK, Malosse C, Davies J, et al. Using gold nanoparticles for enhanced intradermal delivery of poorly soluble auto-antigenic peptides. *Nanomed Nanotechnol Biol Med* 2021; 32: 102321.
131. Liu T, Jiang G, Song G, et al. Fabrication of separable microneedles with phase change coating for NIR-triggered transdermal delivery of metformin on diabetic rats. *Biomed Microdevices* 2020; 22: 12.
132. Mihaylova MM and Shaw RJ. The AMPK signalling pathway coordinates cell growth, autophagy and metabolism. *Nat Cell Biol* 2011; 13: 1016–1023.
133. Di J, Yu J, Wang Q, et al. Ultrasound-triggered noninvasive regulation of blood glucose levels using microgels integrated with insulin nanocapsules. *Nano Res* 2017; 10: 1393–1402.
134. Panda A, Shettar A, Sharma PK, et al. Development of lysozyme loaded microneedles for dermal applications. *Int J Pharm* 2021; 593: 120104.
135. Aung NN, Ngawhirunpat T, Rojanarata T, et al. Enhancement of transdermal delivery of resveratrol using eudragit and polyvinyl pyrrolidone-based dissolving microneedle patches. *J Drug Deliv Sci Tech* 2021; 61: 102284.
136. Panda A, Sharma PK, Shivakumar HN, et al. Nicotine loaded dissolving microneedles for nicotine replacement therapy. *J Drug Deliv Sci Tech* 2021; 61: 102300.
137. Permana AD, Anjani QK, Utomo E, et al. Selective delivery of silver nanoparticles for improved treatment of biofilm skin infection using bacteria-responsive microparticles loaded into dissolving microneedles. *Mater Sci Eng C* 2021; 120: 111786.
138. Wan T, Pan Q and Ping Y. Microneedle-assisted genome editing: A transdermal strategy of targeting NLRP3 by CRISPR-Cas9 for synergistic therapy of inflammatory skin disorders. *Sci Adv* 2021; 7: eabe2888.
139. Peng H, Zhou Y, Zhang C, et al. An accurate and dual-effective body slimming method through a soluble microneedle patch with variable temperature. *J Mater Chem B* 2021; 9: 421–427.
140. Bao C, Li Z, Liang S, et al. Microneedle patch delivery of capsaicin-containing  $\alpha$ -Lactalbumin nanomicelles to adipocytes achieves potent anti-obesity effects. *Adv Funct Mater* 2021; 31: 2011130.
141. GhavamiNejad A, Li J, Lu B, et al. Glucose-responsive composite microneedle patch for hypoglycemia-triggered delivery of native glucagon. *Adv Mater Weinheim* 2019; 31: e1901051.
142. Kim YC, Lee JW, Esser ES, et al. Fabrication of microneedle patches with lyophilized influenza vaccine suspended in organic solvent. *Drug Deliv Transl Res* 2021; 11: 692–701.
143. Koh KJ, Liu Y, Lim SH, et al. Formulation, characterization and evaluation of mRNA-loaded dissolvable polymeric microneedles (RNApatch). *Sci Rep* 2018; 8: 11842.
144. Erdos G, Balmert SC, Carey CD, et al. Improved cutaneous genetic immunization by microneedle array delivery of an adjuvanted adenovirus vaccine. *J Invest Dermatol* 2020; 140: 2528–2531.e2.
145. Yang HW, Ye L, Guo XD, et al. Ebola vaccination using a DNA vaccine coated on PLGA-PLL/ $\gamma$ PGA nanoparticles administered using a microneedle patch. *Adv Healthc Mater* 2017; 6: 1600750.
146. Yenkoidiok-Douti L, Barillas-Mury C and Jewell CM. Design of dissolvable microneedles for delivery of a Pfs47-based malaria transmission-blocking vaccine. *ACS Biomater Sci Eng* 2021; 7: 1854–1862.
147. Vassilieva EV, Li S, Korniyuchuk H, et al. CGAMP/saponin adjuvant combination improves protective response to influenza vaccination by microneedle patch in an aged mouse model. *Front Immunol* 2021; 11: 3630.
148. Yan Q, Cheng Z, Liu H, et al. Enhancement of Ag85B DNA vaccine immunogenicity against tuberculosis by dissolving microneedles in mice. *Vaccine* 2018; 36: 4471–4476.
149. Cole G, Ali AA, McErlean E, et al. DNA vaccination via RALA nanoparticles in a microneedle delivery system induces a potent immune response against the endogenous prostate cancer stem cell antigen. *Acta Biomater* 2019; 96: 480–490.
150. Irvine DJ, Hanson MC, Rakhra K, et al. Synthetic nanoparticles for vaccines and immunotherapy. *Chem Rev* 2015; 115: 11109–11146.
151. Clem AS. Fundamentals of vaccine immunology. *J Glob Infect Dis* 2011; 3: 73–78.
152. Shin MD, Shukla S, Chung YH, et al. COVID-19 vaccine development and a potential nanomaterial path forward. *Nat Nanotechnol* 2020; 15: 646–655.

153. Hossain MK, Ahmed T, Bhusal P, et al. Microneedle systems for vaccine delivery: the story so far. *Expert Rev Vaccines* 2020; 19: 1153–1166.
154. Jain S, Batra H, Yadav P, et al. COVID-19 vaccines currently under preclinical and clinical studies, and associated antiviral immune response. *Vaccines* 2020; 8: 649.
155. Trovato M, Sartorius R, D'Apice L, et al. Viral emerging diseases: challenges in developing vaccination strategies. *Front Immunol* 2020; 11: 2130.
156. Buonaguro L and Tagliamonte M. Selecting target antigens for cancer vaccine development. *Vaccines* 2020; 8: 615.
157. Haniffa M, Gunawan M and Jardine L. Human skin dendritic cells in health and disease. *J Dermatol Sci* 2015; 77: 85–92.
158. Geherin SA, Fintushel SR, Lee MH, et al. The skin, a novel niche for recirculating B cells. *J Immunol* 2012; 188: 6027–6035.
159. Collin M, McGovern N and Haniffa M. Human dendritic cell subsets. *Immunology* 2013; 140: 22–30.
160. Fukunaga A, Khaskhely NM, Sreevidya CS, et al. Dermal dendritic cells, and not Langerhans cells, play an essential role in inducing an immune response. *J Immunol* 2008; 180: 3057–3064.
161. Roh JS and Sohn DH. Damage-associated molecular patterns in inflammatory diseases. *Immune Netw* 2018; 18: e27.
162. Sabado RL, Balan S and Bhardwaj N. Dendritic cell-based immunotherapy. *Cell Res* 2017; 27: 74–95.
163. Ainscough JS, Frank Gerberick G, Dearman RJ, et al. Danger, intracellular signaling, and the orchestration of dendritic cell function in skin sensitization. *J Immunotoxicol* 2013; 10: 223–234.
164. Liu T, Zhang L, Joo D, et al. NF- $\kappa$ B signaling in inflammation. *Signal Transduct Target Ther* 2017; 2(1): 9.
165. Brutkiewicz RR. Cell signaling pathways that regulate antigen presentation. *J Immunol* 2016; 197: 2971–2979.
166. Duong HTT, Yin Y, Thambi T, et al. Smart vaccine delivery based on microneedle arrays decorated with ultra-pH-responsive copolymers for cancer immunotherapy. *Biomaterials* 2018; 185: 13–24.
167. Choi I-J, Na W, Kang A, et al. Patchless administration of canine influenza vaccine on dog's ear using insertion-responsive microneedles (IRMN) without removal of hair and its in vivo efficacy evaluation. *Eur J Pharm Biopharm* 2020; 153: 150–157.
168. Choi I-J, Cha H-R, Hwang SJ, et al. Live vaccinia virus-coated microneedle array patches for smallpox vaccination and stockpiling. *Pharmaceutics* 2021; 13(2): 09.
169. Ho W, Gao M, Li F, et al. Next-generation vaccines: nanoparticle-mediated DNA and mRNA delivery. *Adv Healthc Mater* 2021; 10: e2001812.
170. Duong HTT, Kim NW, Thambi T, et al. Microneedle arrays coated with charge reversal pH-sensitive copolymers improve antigen presenting cells-homing DNA vaccine delivery and immune responses. *J Control Release* 2018; 269: 225–234.
171. Kuwentrai C, Yu J, Rong L, et al. Intradermal delivery of receptor-binding domain of SARS-CoV-2 spike protein with dissolvable microneedles to induce humoral and cellular responses in mice. *Bioeng Transl Med* 2020; 6: e10202.
172. Chen Y-C, Chen S-J, Cheng H-F, et al. Development of Yersinia pestis F1 antigen-loaded liposome vaccine against plague using microneedles as a delivery system. *J Drug Deliv Sci Tech* 2020; 55: 101443.
173. Chang H, Chew SWT, Zheng M, et al. Cryomicroneedles for transdermal cell delivery. *Nat Biomed Eng* 2021; 5: 1008–1018.
174. Wang P, Sun Y, Shi X, et al. Bioscaffolds embedded with regulatory modules for cell growth and tissue formation: a review. *Bioact Mater* 2021; 6: 1283–1307.
175. Zhu Y, Joralmon D, Shan W, et al. 3D printing biomimetic materials and structures for biomedical applications. *Bio-Des Manuf* 2021; 4: 405–428.
176. Tang J, Wang J, Huang K, et al. Cardiac cell-integrated microneedle patch for treating myocardial infarction. *Sci Adv* 2018; 4: eaat9365.
177. Schantz J-T, Chim H and Whiteman M. Cell guidance in tissue engineering: SDF-1 mediates site-directed homing of mesenchymal stem cells within three-dimensional polycaprolactone scaffolds. *Tissue Eng* 2007; 13: 2615–2624.
178. Lee K, Xue Y, Lee J, et al. A patch of detachable hybrid microneedle depot for localized delivery of mesenchymal stem cells in regeneration therapy. *Adv Funct Mater* 2020; 30: 2000086.
179. Jeong S-Y, Park J-H, Lee Y-S, et al. The current status of clinical research involving Microneedles: a systematic review. *Pharmaceutics* 2020; 12(11): 13.
180. Lee KJ, Jeong SS, Roh DH, et al. A practical guide to the development of microneedle systems – in clinical trials or on the market. *Int J Pharm* 2020; 573: 118778.
181. Sharma S, El-Laboudi A, Reddy M, et al. A pilot study in humans of microneedle sensor arrays for continuous glucose monitoring. *Anal Methods* 2018; 10: 2088–2095.
182. Gowers SAN, Freeman DME, Rawson TM, et al. Development of a minimally invasive microneedle-based sensor for continuous monitoring of  $\beta$ -lactam antibiotic concentrations in vivo. *ACS Sens* 2019; 4: 1072–1080.
183. Kolluru C, Williams M, Chae J, et al. Recruitment and collection of dermal interstitial fluid using a microneedle patch. *Adv Healthc Mater* 2019; 8: e1801262.
184. Lee CR, Kim MS, Lee HB, et al. The effect of molecular weight of drugs on transdermal delivery system using microneedle device. *Key Eng Mater* 2007; 342–343: 945–948.
185. Pastorin G, Junginger H, Nayak T, et al. Nanoneedles devices for transdermal vaccine delivery: in vitro and in vivo evaluation. In: *Controlled Release Society*, Copenhagen, Denmark, 2009, pp.18–22.
186. Avcil M and Çelik A. Microneedles in Drug Delivery: Progress and Challenges. *Micromachines* 2021; 12: 1321.
187. Donnelly RF, Singh TRR, Morrow DI, et al. *Microneedle-mediated transdermal and intradermal drug delivery*, Pondicherry, India, 2012.
188. Lee HS, Ryu HR, Roh JY, et al. Bleomycin-coated microneedles for treatment of warts. *Pharm Res* 2017; 34: 101–112.
189. Römgens AM, Bader DL, Bouwstra JA, et al. Monitoring the penetration process of single microneedles with varying tip diameters. *J Mech Behav Biomed Mater* 2014; 40: 397–405.
190. Makvandi P, Kirkby M, Hutton ARJ, et al. Engineering microneedle patches for improved penetration: analysis, skin models and factors affecting needle insertion. *Nano-Micro Lett* 2021; 13: 93.
191. Ramasubramanian MK, Barham OM and Swaminathan V. Mechanics of a mosquito bite with applications to microneedle design. *Bioinspir Biomim* 2008; 3: 046001.